haematologica
Journal of the Ferrata Storti Foundation

Impact of genetic alterations on central nervous system progression of primary vitreoretinal lymphoma

by Kota Yoshifuji, Daichi Sadato, Takashi Toya, Yotaro Motomura, Chizuko Hirama, Hiroshi Takase, Kouhei Yamamoto, Yuka Harada, Takehiko Mori, and Toshikage Nagao

Received: January 1, 2024.
Accepted: May 24, 2024.

Citation: Kota Yoshifuji, Daichi Sadato, Takashi Toya, Yotaro Motomura, Chizuko Hirama, Hiroshi Takase, Kouhei Yamamoto, Yuka Harada, Takehiko Mori, and Toshikage Nagao. Impact of genetic alterations on central nervous system progression of primary vitreoretinal lymphoma. Haematologica. 2024 June 6. doi: 10.3324/haematol.2023.284953 [Epub ahead of print]

Impact of genetic alterations on central nervous system progression of primary vitreoretinal lymphoma

Kota Yoshifuji[1]*, Daichi Sadato[2]*, Takashi Toya[3], Yotaro Motomura[1], Chizuko Hirama[2], Hiroshi Takase[4], Kouhei Yamamoto[5], Yuka Harada[6], Takehiko Mori[1], and Toshikage Nagao[1]

[1]Department of Hematology, Graduate School of Medical and Dental Sciences, Tokyo Medical and Dental University (TMDU), Tokyo, Japan

[2]Clinical Research Support Center, Tokyo Metropolitan Komagome Hospital, Tokyo, Japan

[3] Hematology Division, Tokyo Metropolitan Komagome Hospital, Tokyo, Japan

[4]Department of Ophthalmology & Visual Science, Graduate School of Medical and Dental Sciences, Tokyo Medical and Dental University (TMDU), Tokyo, Japan

[5]Department of Pathology, Graduate School of Medical and Dental Sciences, Tokyo Medical and Dental University (TMDU), Tokyo, Japan

[6] Clinical Laboratory, Tokyo Metropolitan Komagome Hospital, Tokyo, Japan

Running head: Genetic alterations affect CNS progression of PVRL

Corresponding author: Kota Yoshifuji

E-mail: yoshhema@tmd.ac.jp

Contributions

KYo and DS designed the study. KYo, YM, and HT collected the clinical data. HT and KYa collected the clinical samples. KYo, DS, TT, CH, and TN carried out the research and analyzed the data. KYo, DS, TT, and TN wrote the manuscript and designed the figures and tables. HT, YH, TM, and TN supervised the project. All authors approved the final manuscript.

*KYo and DS contributed equally as first coauthors.

Data sharing statement: Requests for original data should be emailed to yoshhema@tmd.ac.jp

Acknowledgments

The authors thank Enago (https://www.enago.com/) for English language editing.

Funding: This work was supported by JSPS KAKENHI (grant numbers JP22K20785, JP23K15296, and JP22K09763).

Disclosures: The authors declare no competing financial interests.

Abstract

Primary vitreoretinal lymphoma (PVRL) is a rare malignant lymphoma subtype with an unfavorable prognosis due to frequent central nervous system (CNS) progression. Thus, identifying factors associated with CNS progression is essential for improving the prognosis of PVRL patients. Accordingly, we conducted a comprehensive genetic analysis using archived vitreous humor samples of 36 PVRL patients diagnosed and treated at our institution and retrospectively examined the relationship between genetic alterations and CNS progression. Whole-exome sequencing (n = 2) and amplicon sequencing using a custom panel of 107 lymphomagenesis-related genes (n = 34) were performed to assess mutations and copy number alterations. The median number of pathogenic genetic alterations per case was 12 (range: 0–22). Pathogenic genetic alterations of *CDKN2A*, *MYD88*, *CDKN2B*, *PRDM1*, *PIM1*, *ETV6*, *CD79B*, and *IGLL5*, as well as aberrant somatic hypermutations, were frequently detected. The frequency of *ETV6* loss and *PRDM1* alteration (mutation and loss) was 23% and 49%, respectively. Multivariate analysis revealed *ETV6* loss (hazard ratio [HR]: 3.26, 95% confidence interval [CI]: 1.08–9.85) and *PRDM1* alteration (HR: 2.52, 95% CI: 1.03–6.16) as candidate risk factors associated with CNS progression of PVRL. Moreover, these two genetic factors defined slow-, intermediate-, and rapid-progression groups (0, 1, and 2 factors, respectively), and the median period to CNS progression differed significantly among them (52 vs. 33 vs. 20 months, respectively). Our findings suggest that genetic factors predict the CNS progression of PVRL effectively, and the genetics-based CNS progression model might lead to stratification of treatment.

Introduction

Primary vitreoretinal lymphoma (PVRL) is a malignant lymphoma subtype with lesions limited to the vitreous humor, retina, and optic nerve.[1] The pathological classification of PVRL is typically diffuse large B-cell lymphoma (DLBCL)[2] with *MYD88* L265P and/or *CD79B* mutations.[3, 4]

Intravitreal chemotherapy, such as methotrexate (MTX), and local radiotherapy have been reported to achieve intraocular complete response and improve visual symptoms.[5-7] Additionally, systemic chemotherapy is often administered following local treatment in an effort to prevent subsequent central nervous system (CNS) progression. We previously reported a single-arm prospective study on newly diagnosed PVRL patients who received an intravitreal MTX injection followed by systemic high-dose MTX (HD-MTX). All patients achieved intraocular complete response, and the adverse events were generally tolerable.[8] However, the high rate of CNS progression indicated that these prophylactic strategies did not improve PVRL prognosis.[9, 10] Therefore, the identification of factors associated with CNS progression is essential to improve the prognosis of PVRL patients.

In recent years, comprehensive genetic analyses using next-generation sequencing have revealed numerous genetic alterations in systemic DLBCL and provided solid evidence to newly classify DLBCL based on genetic alterations[11-13]; PVRL is classified into MCD/cluster 5 subtype with *MYD88* and *CD79B* mutations. Furthermore, genetic subtype-guided immunochemotherapy was reported to show better efficacy than conventional chemotherapy in DLBCL.[14, 15] Thus, this genetic approach is expected to be applied in clinical settings, such as exploring new target therapies and prognostic stratification.

We recently performed a retrospective analysis of PVRL patients diagnosed and treated at our hospital to identify the clinical factors associated with CNS progression, revealing bilateral disease and the detection of B-cell clonality confirmed via flow cytometry at diagnosis as risk factors.[16] Previously, we conducted direct sequencing and allele-specific polymerase chain reaction (PCR) to check the mutation of *CD79B* Y196 and *MYD88* L265P on the archived vitreous humor samples from 17 patients with PVRL and argued that *CD79B* Y196 potentially has a prognostic potential for patients with PVRL.[3] In the present study, we performed a comprehensive and massive genetic analysis of archived vitreous humor samples from 36 PVRL patients to identify genetic alterations strongly associated with CNS progression.

Methods

Patients

We enrolled 36 PVRL patients diagnosed from April 2012 to March 2022 who were treated at our hospital and had archived vitreous humor samples. Some of them had been included in previous studies,[3, 8, 16] and 8 of 36 patients herein were identical to those in the previous study[3]. PVRL was defined as VRL localized to the eyes and was diagnosed as previously described.[8, 9, 16] Details of PVRL patients in this study are shown in Figure 1. The methods of FCM analysis, PCR analysis of *IGH* rearrangement, and cytokine measurement were previously described[3, 8] and shown in the Supplemental Method. Treatment for the patients were also described in Supplemental Method.

This study was performed in accordance with the Declaration of Helsinki and approved by the Ethics Committee of Tokyo Medical and Dental University (approval number: M2017-341). All patients provided written informed consent.

DNA extraction and next-generation sequencing

Genomic DNA was extracted from vitreous humor or from formalin-fixed paraffin-embedded (FFPE) brain tissue biopsies of PVRL patients using an EZ1 Virus Mini Kit v2.0 (QIAGEN, Hilden, Germany) or a QIAamp DNA FFPE Advanced Kit (QIAGEN), respectively. EZ1 Virus Mini Kit v2.0 usually extracts cell-free DNA; however, Zong et al. reported,[17] that genomic DNA with enough quality and quantity was extracted from cells. Library preparation for amplicon-based targeted sequencing was performed as previously described[18] using a custom gene panel of 107 genes frequently mutated in lymphoma, particularly in PVRL (Table S1). Briefly, the library was prepared using AmpliSeq Library Plus for Illumina (Illumina, San Diego, CA, USA). Further, synthesized libraries were sequenced in Miseq (Illumina) paired-end runs. The details of library synthesis method are described in the Supplemental Method.

Gene alteration analysis

We used a mutational analysis pipeline based on previously reported method.[18] The data handling step and used tools were described in the Supplemental Method. Variants considered pathogenic were

identified according to previous reports (Table S1). We also identified and counted aberrant somatic hypermutation (aSHM) to specify hypermutated cases, although their pathogenicity could not be determined. Copy number alterations (CNA) were calculated based on a previously described method.[19] Detection methods of CNA were described in the Supplemental Method in detail.

Statistical analysis

Fisher exact test was used for categorical variable analysis and Mann–Whitney U test for continuous variable analysis. The cumulative incidence of CNS progression was calculated in the presence of death as a competing event, and the difference was tested using Gray test, although all PVRL patients who died had CNS progression before death. Factors used for the multivariate analysis were selected using the stepwise Akaike information criterion (AIC) method from the factors that revealed significant differences in the univariate analysis. Multivariate analysis was performed using Fine and Gray proportional hazard modeling. AIC was used as the selection criteria. All statistical analyses were performed using R 4.2.0 software (The R Foundation for Statistical Computing), and statistical significance was defined as $p < 0.05$ based on a two-sided test.

Results

Patient characteristics

We evaluated 36 patients diagnosed with PVRL. The median follow-up period was 29 months (range: 2–119 months). Patient characteristics are summarized in Table 1. Ocular involvement was unilateral in 16 and bilateral in 20 patients. The median time from the onset of initial visual symptoms to diagnosis was 8 months (range: 1–29 months). Cytopathology, flow cytometry analysis, and *IGH* rearrangement were positive for PVRL in 42%, 74%, and 80% of patients, respectively. All 36 patients received intravitreal MTX injections following PVRL diagnosis, and 20/36 patients were treated with systemic HD-MTX thereafter. During the observation period, 19 patients developed CNS progression. Among the patients suspected with PVRL, one patient had CNS progression and ocular relapse, and one patient had ocular relapse.

Landscape of pathogenic genetic alterations in PVRL

Whole-exome sequencing (n = 2) and amplicon sequencing using a custom panel containing 107 lymphomagenesis-related genes (n = 34) were performed on vitreous humor samples to assess mutations and CNA. Coverage depths of whole-exome sequencing were 105.8 and 143.5, and the mean coverage depth of amplicon sequencing was 621.8 (range: 74.77–1,098). One sample had low-quality DNA and could not be evaluated for CNA. The detected pathogenic gene mutations and CNA are presented in Tables S2 and S3, respectively.

At least one pathogenic genetic alteration was detected in 31/36 samples, and the median number of pathogenic genetic alterations per case was 12 (range: 0–22) (Figure 2A). The landscape of pathogenic genetic alteration is shown in Figure 2B. The top three altered genes were *CDKN2A* (25/36, 69%), *MYD88* (23/36, 64%), and *CDKN2B* (21/36, 58%). Of the 25 cases of altered *CDKN2A*, 23 showed copy number loss, two of which also showed mutation, and mutation only was observed in two cases. All *CDKN2B* alterations were copy number loss, and all *MYD88* alterations were mutations in p.Leu265. The other frequently altered genes were *PRDM1* (47%), *PIM1* (44%), *ETV6* (42%), *CD79B* (42%), and *IGLL5* (42%). In some cases, mutation and copy number loss were observed in the same genes. The cases with gene mutations showing >50% variant allele frequencies in the presence of copy number loss were identified. Considerably, these alterations occurred in different allele, indicating deletion of the normal allele.

Aberrant somatic hypermutation

Activation-induced deaminase mediates SHM and class-switch recombination by converting cytosine residues into uracil residues. aSHM arises from errors during SHM and occurs in genes other than immunoglobulin V such as *PIM1* and *IGLL5*. aSHM is frequently detected in DLBCL, a subtype that accounts for most PVRL cases. However, the association between aSHM and DLBCL initiation has yet to be verified.[20, 21] We picked up eight genes (*PIM1*, *OSBPL10*, *MPEG1*, *IGLL5*, *BTG1*, *BTG2*, *ETV6*, and *IRF4*), which were reportedly related to aSHM and examined the impact of aSHM in our study. Figure 3A shows the number of mutations per gene per case. One or more mutations in *PIM1*, *OSBPL10*, *MPEG1*, *IGLL5*, *BTG1*, *BTG2*, *ETV6*, and *IRF4* were found in 24, 14, 12, 20, 10, 12, 12, and 2 of the 36 PVRL cases, respectively. Figure 3B shows the total number of mutations detected in these eight genes

per case. The median number of mutations per case was 10 (range: 0–35). There was no clear correlation between the number of pathogenic genetic alterations and the number of mutations detected in these eight genes related to aSHM per case.

Genetic risk factors associated with CNS progression

Figure 4A shows the cumulative incidence of CNS progression, and the 5-year cumulative incidence of CNS progression was 78.3%. We investigated possible genetic alterations associated with CNS progression. The univariate analysis identified *CD79B* mutation, *BTG1* mutation, *ETV6* loss, and *PRDM1* alteration (mutation and copy number loss) as candidate risk factors (Table 2). Factors used for the multivariate analysis were selected using the stepwise AIC method from these four factors, and *CD79B* mutation was excluded. *ETV6* loss and *PRDM1* alteration remained significant in the multivariate analysis (Table 2). The number of pathogenic genetic alterations and the number of mutations detected in eight genes related to aSHM were not associated with CNS progression. We also investigated the association between *ETV6* loss/*PRDM1* alteration and clinical findings of PVRL, but there was no significant correlation (Tables S4 and S5, respectively).

Genetic model of CNS progression in PVRL

ETV6 loss and *PRDM1* alteration were identified as risk factors for CNS progression in PVRL. We created a genetics-based CNS progression model using these two factors to define the slow-, intermediate-, and rapid-progression groups (0, 1, and 2 factors, respectively) (Figure 4B). The median period to CNS progression differed significantly among the three groups (52 vs. 33 vs. 20 months, respectively).

Genetic comparison between primary vitreous humor and brain samples

CNS progression occurred in 19/36 PVRL patients, four of whom underwent brain biopsy, and the tissue was processed using FFPE. The genetic-based group of the four patients was two in the intermediate-progression group and one in the slow- and rapid-progression groups. The period of CNS progression was 39 months (slow-progression group), 11 and 32 months (intermediate-progression group), and 20 months (rapid-progression group). We performed amplicon sequencing and analysis to compare pathogenic

genetic alterations in the brain tissue samples with those in the vitreous humor samples taken at diagnosis. All four patients had at least one concordant alteration and had additional alterations that were found in the brain tissue samples but not in the vitreous humor samples (Figure 5). Details of detected pathogenic gene mutations and CNA in the brain tissue and vitreous humor samples are presented in Table S6.

Discussion

We conducted a comprehensive genetic analysis of 36 PVRL patients using vitreous humor samples taken at diagnosis and determined the genetic alterations related to CNS progression in PVRL.

Mutation and copy number analyses revealed that pathogenic genetic alterations of *CDKN2A*, *MYD88*, *CDKN2B*, *PRDM1*, *PIM1*, *ETV6*, *CD79B*, and *IGLL5* were common, as well as aSHM in *PIM1*, *OSBPL10*, *MPEG1*, *IGLL5*, *BTG1*, and *BTG2*. Due to the rarity of PVRL, comprehensive genetic analysis is challenging, and this is compounded by the low quantity and quality of DNA extracted from vitreous humor samples. However, a few groups have recently published exciting reports in this context using small amounts of DNA or cell-free DNA.[22-25] Because the results of our genetic analysis were highly consistent with the results of these comprehensive studies, we considered them suitable for the analysis of genetic alterations predictive of CNS progression in PVRL. Notably, there were 36 participants in our study, which is more than previous genetic analyses of PVRL.

We identified *ETV6* loss and *PRDM1* alteration (mutation and copy number loss) as candidate genetic alterations predicting CNS progression in PVRL. Our study is the first comprehensive genetic analysis to imply the association of genetic risk factors with CNS involvement. Thus, our findings stand out in terms of novelty.

ETV6 is a transcriptional repressor that plays a crucial role in hematopoiesis and is related to various types of hematological malignancies, including DLBCL.[11, 26-28] *ETV6* loss, mutation, and fusion have been reported in primary central nervous system lymphoma (PCNSL).[29-31] This is consistent with our finding that *ETV6* loss is a factor related to CNS progression in PVRL, although the precise mechanism remains unclear. Notably, the level of ETV6 protein expression is negatively correlated with BIRC5 (survivin) expression and is associated with the antitumor effect of YM155, a BIRC5-specific inhibitor.[32] YM155 has shown clinical efficacy as a single agent or in combination with rituximab or bendamustine to

treat relapsed/refractory DLBCL.[33, 34] Future studies on the effectiveness of YM155 treatment for PVRL and its association with *ETV6* loss are anticipated.

PRDM1 is also a transcriptional repressor and a key molecule involved in plasma cell differentiation.[35] *PRDM1* mutation and loss are frequently detected in activated B-cell–like (ABC) DLBCL,[11] and conditional knockout of *PRDM1* in B cells results in constitutive NF-κB activation and the development of lymphoproliferative disorders resembling ABC-DLBCL in vivo.[36] Genetic alteration of *PRDM1* frequently occurs in PCNSL.[29] Although the precise mechanism of CNS progression remains undefined, considering that *PRDM1* alterations are infrequent in systemic extranodal DLBCL,[37, 38] there may be a CNS-specific genetic pathogenesis. Bruton tyrosine kinase (BTK) inhibitors interfere with B-cell receptor and NF-κB signaling by inhibiting BTK, and ibrutinib (a BTK inhibitor) has shown encouraging clinical activity against lymphomas involving the CNS and intraocular sites.[39] Thus, it would be interesting to investigate whether the presence or absence of genetic alterations in *PRDM1* affects BTK inhibitor efficacy. Moreover, Pascual et al. reported that constitutive NF-κB activation and impaired differentiation resulting from Blimp1 (a PRDM1 homolog) inactivation downregulated p53 signaling and triggered immune escape in ABC-DLBCL and that simultaneous PD-1 blockade improved the efficacy of anti-CD20 immunotherapy in an ABC-DLBCL-like mouse model.[40] In parallel, since the efficacy of PD-1 blockade for CNS lymphoma has been reported,[41, 42] immune checkpoint modulation for PVRL patients with *PRDM1* alteration may be an intriguing therapeutic approach.

The genetics-based CNS progression model that we proposed in this study used two genetic alterations, namely, *ETV6* loss and *PRDM1* alterations, to successfully define three statistically significant groups for CNS progression in PVRL patients. To break through this intractable lymphoma, therapeutic strategies should be adapted using conventional HD-MTX-based chemotherapy regimens in potential combination with novel agents, such as BTK inhibitors, to the CNS progression risk of each patient. Our genetics-based CNS progression model might help this stratified treatment.

Since a comparison between the genetic alterations in PVRL at disease onset and after CNS progression had never been reported, we performed a longitudinal comparison of pathogenic genetic alterations identified using amplicon sequencing of FFPE brain tissue samples from four PVRL patients with CNS progression and their vitreous humor samples at diagnosis. All four patients with PVRL had at least one concordant alteration. Balikov et al. conducted target sequencing of matched brain and vitreous samples

in two PCNSL patients with VRL and showed shared genetic alterations, suggesting the same origin.[43] Similarly, our results described that brain lesions were of the same origin as the vitreous lesions at diagnosis. Moreover, all four patients had additional pathogenic genetic alterations that were absent at disease onset. Thus, future analysis with a larger number of PVRL patients may facilitate the identification of additional genetic alterations associated with CNS lesion development.

This study has some limitations. First, as a single-institute, retrospective analysis, selection bias cannot be ignored. Second, although we considered the number of lymphomagenesis-related genes (n = 107) examined in the amplicon sequences sufficient to cover most genetic alterations in the context of PVRL, it is possible that other (untested) genetic alterations are involved in CNS progression. Third, although our study enrolled 36 PVRL patients, which is the largest in number to date for a comprehensive genetic analysis of this rare disease, the sample size was small. During the analysis of rare diseases, the small sample size might reduce the power of detection[44]. Therefore, we did not use multiplicity correction methods for the results of regression tests because they further reduced the detection power. Studies with large sample sizes using multiple comparison correction methods in multivariate analysis will enable a detailed investigation of the biological characteristics of PVRL. Finally, we could not validate our results in another cohort. We seek to test the validity of this genetics-based CNS progression model in a prospective and large cohort through international collaborations in the future.

To summarize, our comprehensive genetic analysis identified *ETV6* loss and *PRDM1* alterations as candidate genetic risk factors related to CNS progression in PVRL. Subsequently, we created a new model for CNS progression using these two genetic risk factors. A prospective and large study is necessary to validate this model. With proven validity, interventions with new drugs targeting these genetic alterations in possible combination with other available therapeutic options based on this model may improve the outcome of PVRL.

References

1. Soussain C, Malaise D, Cassoux N. Primary vitreoretinal lymphoma: a diagnostic and management challenge. Blood. 2021;138(17):1519-1534.

2. Chan CC, Rubenstein JL, Coupland SE, et al. Primary vitreoretinal lymphoma: a report from an International Primary Central Nervous System Lymphoma Collaborative Group symposium. Oncologist. 2011;16(11):1589-1599.

3. Yonese I, Takase H, Yoshimori M, et al. CD79B mutations in primary vitreoretinal lymphoma: Diagnostic and prognostic potential. Eur J Haematol. 2019;102(2):191-196.

4. Raja H, Salomão DR, Viswanatha DS, Pulido JS. Prevalence of MYD88 L265P mutation in histologically proven, diffuse large B-cell vitreoretinal lymphoma. Retina. 2016;36(3):624-628.

5. Fishburne BC, Wilson DJ, Rosenbaum JT, Neuwelt EA. Intravitreal methotrexate as an adjunctive treatment of intraocular lymphoma. Arch Ophthalmol. 1997;115(9):1152-1156.

6. Habot-Wilner Z, Frenkel S, Pe'er J. Efficacy and safety of intravitreal methotrexate for vitreo-retinal lymphoma - 20 years of experience. Br J Haematol. 2021;194(1):92-100.

7. Ferreri AJ, Blay JY, Reni M, et al. Relevance of intraocular involvement in the management of primary central nervous system lymphomas. Ann Oncol. 2002;13(4):531-538.

8. Akiyama H, Takase H, Kubo F, et al. High-dose methotrexate following intravitreal methotrexate administration in preventing central nervous system involvement of primary intraocular lymphoma. Cancer Sci. 2016;107(10):1458-1464.

9. Takase H, Arai A, Iwasaki Y, et al. Challenges in the diagnosis and management of vitreoretinal lymphoma - Clinical and basic approaches. Prog Retin Eye Res. 2022;90:101053.

10. Castellino A, Pulido JS, Johnston PB, et al. Role of systemic high-dose methotrexate and combined approaches in the management of vitreoretinal lymphoma: A single center experience 1990-2018. Am J Hematol. 2019;94(3):291-298.

11. Schmitz R, Wright GW, Huang DW, et al. Genetics and Pathogenesis of Diffuse Large B-Cell Lymphoma. N Engl J Med. 2018;378(15):1396-1407.

12. Chapuy B, Stewart C, Dunford AJ, et al. Author Correction: Molecular subtypes of diffuse large B cell lymphoma are associated with distinct pathogenic mechanisms and outcomes. Nat Med. 2018;24(8):1290-1291.

13. Wright GW, Huang DW, Phelan JD, et al. A Probabilistic Classification Tool for Genetic Subtypes of Diffuse Large B Cell Lymphoma with Therapeutic Implications. Cancer Cell. 2020;37(4):551-568.e14.

14. Wilson WH, Wright GW, Huang DW, et al. Effect of ibrutinib with R-CHOP chemotherapy in genetic subtypes of DLBCL. Cancer Cell. 2021;39(12):1643-1653.

15. Zhang MC, Tian S, Fu D, et al. Genetic subtype-guided immunochemotherapy in diffuse large B cell lymphoma: The randomized GUIDANCE-01 trial. Cancer Cell. 2023;41(10):1705-1716.

16. Motomura Y, Yoshifuji K, Tachibana T, et al. Clinical factors for central nervous system progression and survival in primary vitreoretinal lymphoma. Br J Haematol. 2024;204(4):1279-1287.
17. Zong Y, Kamoi K, Kurozumi-Karube H, Zhang J, Yang M, Ohno-Matsui K. Safety of intraocular anti-VEGF antibody treatment under in vitro HTLV-1 infection. Front Immunol. 2022;13:1089286.
18. Sadato D, Hirama C, Kaiho-Soma A, et al. Archival bone marrow smears are useful in targeted next-generation sequencing for diagnosing myeloid neoplasms. PLoS One. 2021;16(7):e0255257.
19. Nagao T, Yoshifuji K, Sadato D, et al. Establishment and characterization of a new activated B-cell-like DLBCL cell line, TMD12. Exp Hematol. 2022;116:37-49.
20. Pasqualucci L, Neumeister P, Goossens T, et al. Hypermutation of multiple proto-oncogenes in B-cell diffuse large-cell lymphomas. Nature. 2001;412(6844):341-346.
21. Pasqualucci L, Bhagat G, Jankovic M, et al. AID is required for germinal center-derived lymphomagenesis. Nat Genet. 2008;40(1):108-112.
22. Wang X, Su W, Gao Y, et al. A pilot study of the use of dynamic cfDNA from aqueous humor and vitreous fluid for the diagnosis and treatment monitoring of vitreoretinal lymphomas. Haematologica. 2022;107(9):2154-2162.
23. Bonzheim I, Sander P, Salmerón-Villalobos J, et al. The molecular hallmarks of primary and secondary vitreoretinal lymphoma. Blood Adv. 2022;6(5):1598-1607.
24. Lee J, Kim B, Lee H, et al. Whole exome sequencing identifies mutational signatures of vitreoretinal lymphoma. Haematologica. 2020;105(9):e458-460.
25. Cani AK, Hovelson DH, Demirci H, Johnson MW, Tomlins SA, Rao RC. Next generation sequencing of vitreoretinal lymphomas from small-volume intraocular liquid biopsies: new routes to targeted therapies. Oncotarget. 2017;8(5):7989-7998.
26. Ford AM, Palmi C, Bueno C, et al. The TEL-AML1 leukemia fusion gene dysregulates the TGF-beta pathway in early B lineage progenitor cells. J Clin Invest. 2009;119(4):826-836.
27. Zhang J, Ding L, Holmfeldt L, et al. The genetic basis of early T-cell precursor acute lymphoblastic leukaemia. Nature. 2012;481(7380):157-163.
28. Alexander TB, Gu Z, Iacobucci I, et al. The genetic basis and cell of origin of mixed phenotype acute leukaemia. Nature. 2018;562(7727):373-379.
29. Radke J, Ishaque N, Koll R, et al. The genomic and transcriptional landscape of primary central nervous system lymphoma. Nat Commun. 2022;13(1):2558.
30. Bruno A, Boisselier B, Labreche K, et al. Mutational analysis of primary central nervous system lymphoma. Oncotarget. 2014;5(13):5065-5075.
31. Chapuy B, Roemer MG, Stewart C, et al. Targetable genetic features of primary testicular and primary central nervous system lymphomas. Blood. 2016;127(7):869-881.

32. Marino D, Pizzi M, Kotova I, et al. High ETV6 Levels Support Aggressive B Lymphoma Cell Survival and Predict Poor Outcome in Diffuse Large B-Cell Lymphoma Patients. Cancers (Basel). 2022;14(2):338.

33. Cheson BD, Bartlett NL, Vose JM, et al. A phase II study of the survivin suppressant YM155 in patients with refractory diffuse large B-cell lymphoma. Cancer. 2012;118(12):3128-3134.

34. Kaneko N, Mitsuoka K, Amino N, et al. Combination of YM155, a survivin suppressant, with bendamustine and rituximab: a new combination therapy to treat relapsed/refractory diffuse large B-cell lymphoma. Clin Cancer Res. 2014;20(7):1814-1822.

35. Shaffer AL, Lin KI, Kuo TC, et al. Blimp-1 orchestrates plasma cell differentiation by extinguishing the mature B cell gene expression program. Immunity. 2002;17(1):51-62.

36. Mandelbaum J, Bhagat G, Tang H, et al. BLIMP1 is a tumor suppressor gene frequently disrupted in activated B cell-like diffuse large B cell lymphoma. Cancer Cell. 2010;18(6):568-579.

37. Li P, Chai J, Chen Z, et al. Genomic Mutation Profile of Primary Gastrointestinal Diffuse Large B-Cell Lymphoma. Front Oncol. 2021;11:622648.

38. de Groen RAL, van Eijk R, Böhringer S, et al. Frequent mutated B2M, EZH2, IRF8, and TNFRSF14 in primary bone diffuse large B-cell lymphoma reflect a GCB phenotype. Blood Adv. 2021;5(19):3760-3775.

39. Soussain C, Choquet S, Blonski M, et al. Ibrutinib monotherapy for relapse or refractory primary CNS lymphoma and primary vitreoretinal lymphoma: Final analysis of the phase II 'proof-of-concept' iLOC study by the Lymphoma study association (LYSA) and the French oculo-cerebral lymphoma (LOC) network. Eur J Cancer. 2019;117:121-130.

40. Pascual M, Mena-Varas M, Robles EF, et al. PD-1/PD-L1 immune checkpoint and p53 loss facilitate tumor progression in activated B-cell diffuse large B-cell lymphomas. Blood. 2019;133(22):2401-2412.

41. Nayak L, Iwamoto FM, LaCasce A, et al. PD-1 blockade with nivolumab in relapsed/refractory primary central nervous system and testicular lymphoma. Blood. 2017;129(23):3071-3073.

42. Ambady P, Szidonya L, Firkins J, et al. Combination immunotherapy as a non-chemotherapy alternative for refractory or recurrent CNS lymphoma. Leuk Lymphoma. 2019;60(2):515-518.

43. Balikov DA, Hu K, Liu CJ, et al. Comparative Molecular Analysis of Primary Central Nervous System Lymphomas and Matched Vitreoretinal Lymphomas by Vitreous Liquid Biopsy. Int J Mol Sci. 2021;22(18):9992.

44. Button KS, Ioannidis JP, Mokrysz C, et al. Power failure: why small sample size undermines the reliability of neuroscience. Nat Rev Neurosci. 2013;14(5):365-376.

Table 1. Patient characteristics at primary vitreoretinal lymphoma diagnosis (N = 36)

Characteristic	Value
Age, median (range), years	71 (43-84)
Sex, male/female	14/22
Laterality, unilateral/bilateral	16/20
Initial visual symptoms	
Blurred vision	20/36 (56%)
Decreased vision	11/36 (31%)
Floaters	6/36 (17%)
Photopsia	1/36 (3%)
Sites involved	
Vitreous body	34/36 (94%)
Retina or subretinal site	18/36 (50%)
Optic nerve	1/36 (3%)
Time to diagnosis, median (range), months	8 (1–29)
Cytopathology positive (class ≥IV)	15/36 (42%)
B-cell clonality (FCM analysis)	23/31 (74%)
Positive for *IGH* rearrangement (PCR)	28/35 (80%)
Cytokine levels in the vitreous humor	
IL-10 (pg/mL), median (range)	993.5 (10–130,125)
IL-10/IL-6 ratio (>1)	33/36 (92%)
Treatment received	
Intravitreal MTX injection alone*	16/36 (44%)
Intravitreal MTX injection + systemic HD-MTX	20/36 (56%)

*Two patients received additional local radiation therapy.

Abbreviations: FCM, flow cytometry; HD-MTX, high-dose methotrexate; IL, interleukin; MTX, methotrexate; PCR, polymerase chain reaction

Table 2. Genetic risk factors for central nervous system progression

Risk factor	**Univariate analysis (p-value)**	**Multivariate analysis (p-value)**	**HR (95% CI)**
CD79B mutation	0.03		
BTG1 mutation	0.01	0.08	2.31 (0.92–5.83)
ETV6 loss	0.04	0.04	3.26 (1.08—9.85)
PRDM1 alteration (mutation + loss)	0.04	0.04	2.52 (1.03–6.16)

p-values < 0.05 were considered statistically significant.

Abbreviations: CI, confidence interval; HR, hazard ratio

Figure legends

Figure 1. Classification of primary vitreoretinal lymphoma (PVRL) patients in this study. *:vitreous humor opacity and/or retinal or subretinal proliferative lesions. FCM, flow cytometry; PCR, polymerase chain reaction; IL, interleukin.

Figure 2. Pathogenic genetic alterations in primary vitreoretinal lymphoma (PVRL). (A) Number of pathogenic genetic alterations per PVRL case. (B) Landscape of pathogenic genetic alterations in PVRL cases. Each column represents a case, and each row represents a recurrently altered gene. The bar graph on the right represents the frequency of pathogenic genetic alteration in each gene.

Figure 3. Aberrant somatic hypermutations (aSHM) of primary vitreoretinal lymphoma. (A) Number of mutations per gene per case. Each dot represents a case. (B) Total number of mutations detected in these eight genes per case. The order of cases in the column is the same as in Figure 2A.

Figure 4. Genetic model of central nervous system (CNS) progression in primary vitreoretinal lymphoma (PVRL). (A) Cumulative incidence of CNS progression in PVRL. (B) Genetic model using *ETV6* loss and *PRDM1* alteration to define slow-, intermediate-, and rapid-progression groups (0, 1, and 2 factors, respectively). Cumulative incidence of CNS progression in the three groups is shown.

Figure 5. Genetic alterations at initial onset and after central nervous system (CNS) progression. Number of pathogenic genetic alterations in vitreous humor samples taken at disease onset and brain tissue biopsy samples taken after CNS progression per case. Concordant alterations (found in both vitreous humor and brain tissue) and discordant alterations (found in either vitreous humor or brain tissue) are indicated.

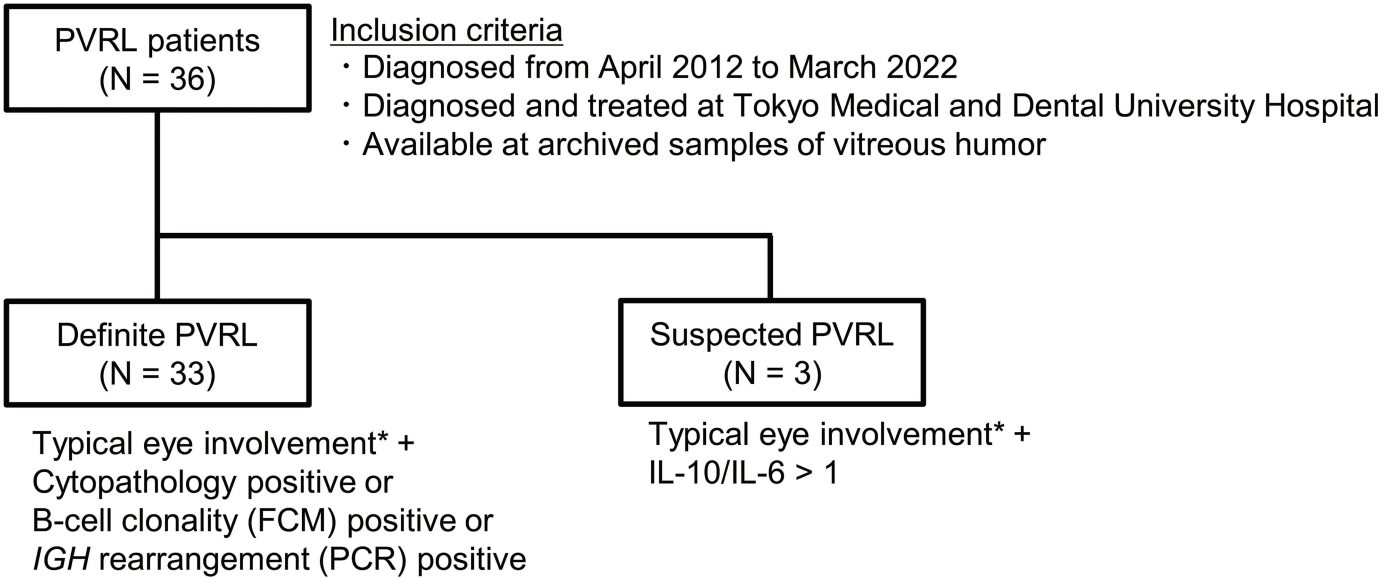
PVRL patients
(N = 36)
Inclusion criteria
・Diagnosed from April 2012 to March 2022
・Diagnosed and treated at Tokyo Medical and Dental University Hospital
・Available at archived samples of vitreous humor
Definite PVRL
(N = 33)
Typical eye involvement* +
Cytopathology positive or
B-cell clonality (FCM) positive or
IGH rearrangement (PCR) positive
Suspected PVRL
(N = 3)
Typical eye involvement* +
IL-10/IL-6 > 1

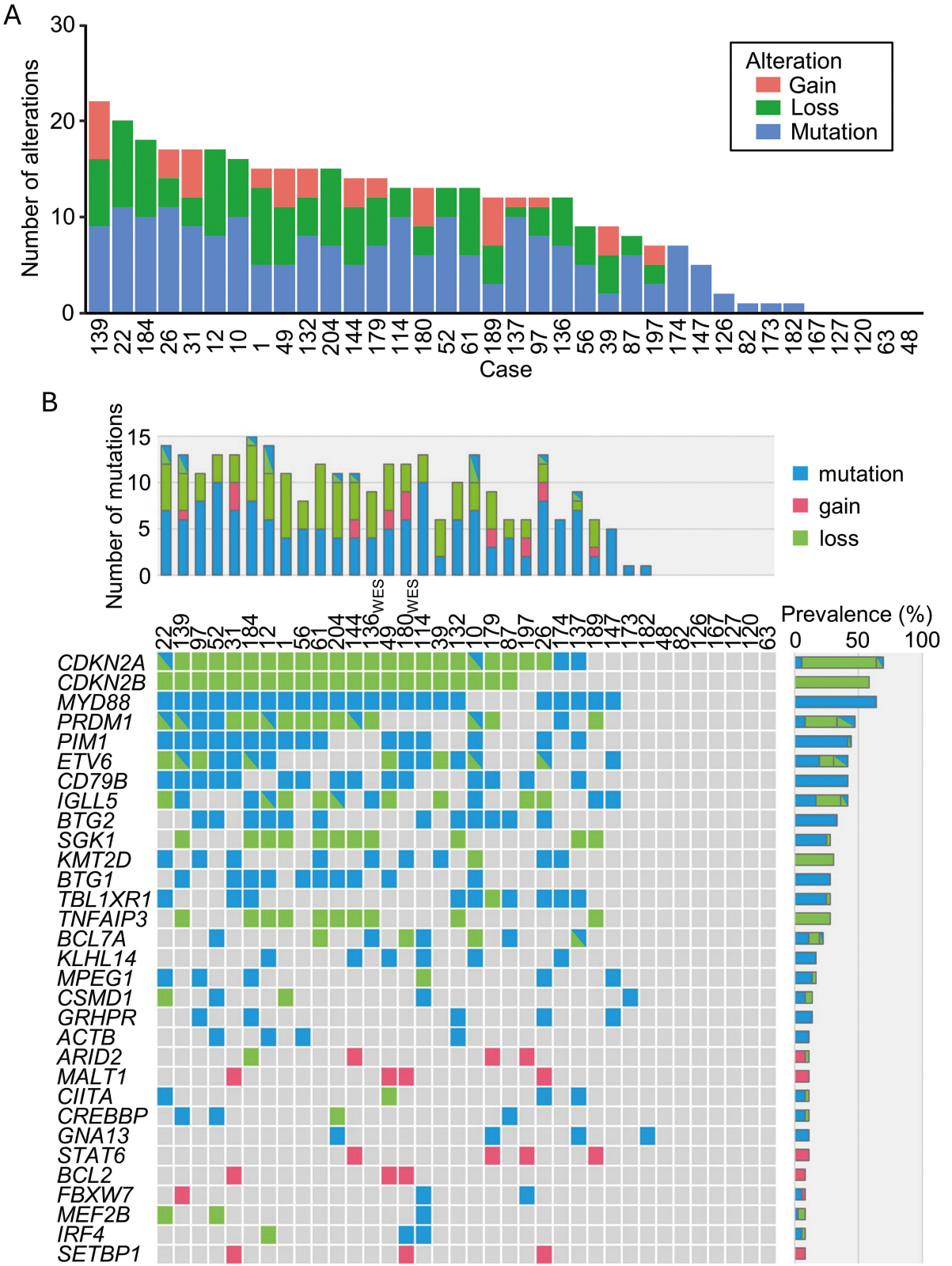
A
Number of alterations
30
20
10
0
Alteration
Gain
Loss
Mutation
139 22 184 26 31 12 10 1 49 132 204 144 179 114 180 52 61 189 137 97 136 56 39 87 197 174 147 126 82 173 182 167 127 120 63 48
Case
B
Number of mutations
15
10
5
0
mutation
gain
loss
WES
WES
Prevalence (%)
0 50 100
22 139 97 52 31 184 12 1 56 61 204 144 136 49 180 114 39 132 10 179 87 197 26 174 137 189 147 173 182 48 82 126 167 120 63
CDKN2A
CDKN2B
MYD88
PRDM1
PIM1
ETV6
CD79B
IGLL5
BTG2
SGK1
KMT2D
BTG1
TBL1XR1
TNFAIP3
BCL7A
KLHL14
MPEG1
CSMD1
GRHPR
ACTB
ARID2
MALT1
CIITA
CREBBP
GNA13
STAT6
BCL2
FBXW7
MEF2B
IRF4
SETBP1

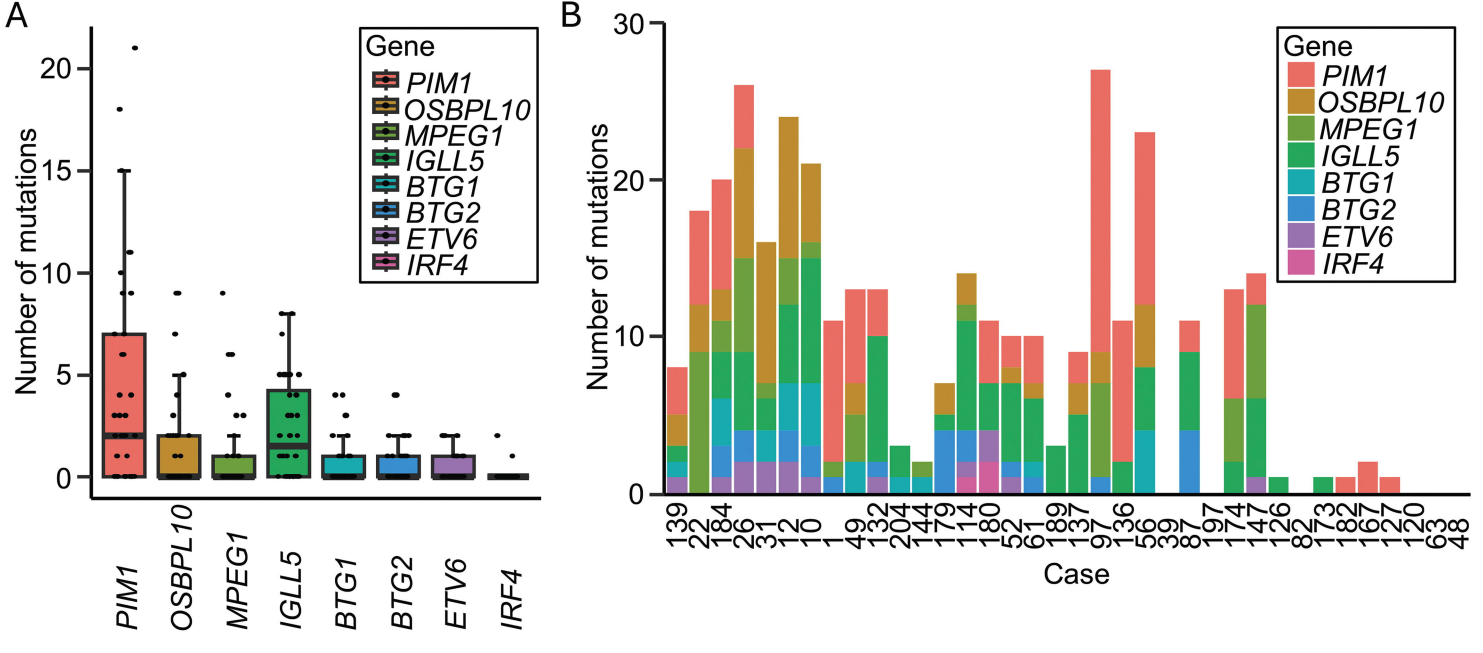
A
Number of mutations
0
5
10
15
20
Gene
PIM1
OSBPL10
MPEG1
IGLL5
BTG1
BTG2
ETV6
IRF4
PIM1
OSBPL10
MPEG1
IGLL5
BTG1
BTG2
ETV6
IRF4
B
Number of mutations
0
10
20
30
Gene
PIM1
OSBPL10
MPEG1
IGLL5
BTG1
BTG2
ETV6
IRF4
139 22 184 26 31 12 10 1 49 132 204 144 179 114 180 52 61 189 137 97 136 56 39 87 197 174 147 126 82 173 182 167 127 120 63 48
Case

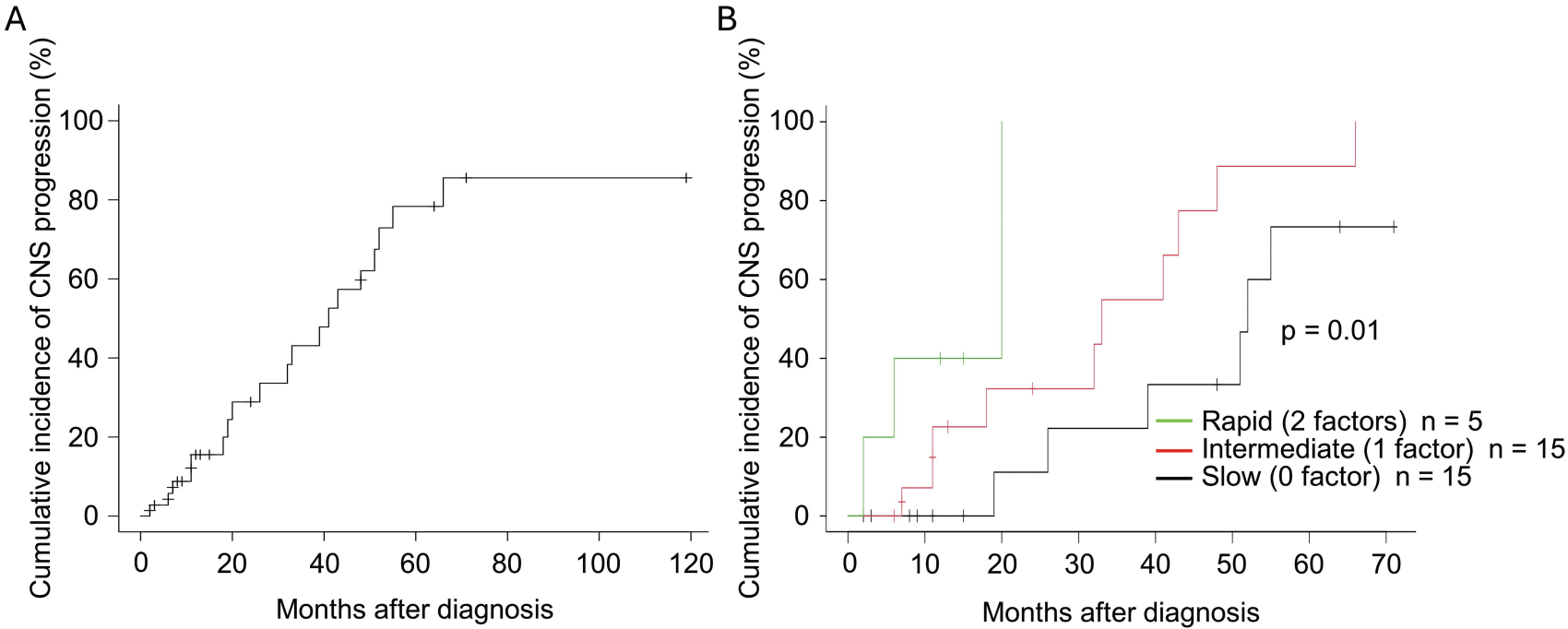
A
Cumulative incidence of CNS progression (%)
100
80
60
40
20
0
0
20
40
60
80
100
120
Months after diagnosis
B
Cumulative incidence of CNS progression (%)
100
80
60
40
20
0
0
10
20
30
40
50
60
70
Months after diagnosis
p = 0.01
Rapid (2 factors) n = 5
Intermediate (1 factor) n = 15
Slow (0 factor) n = 15

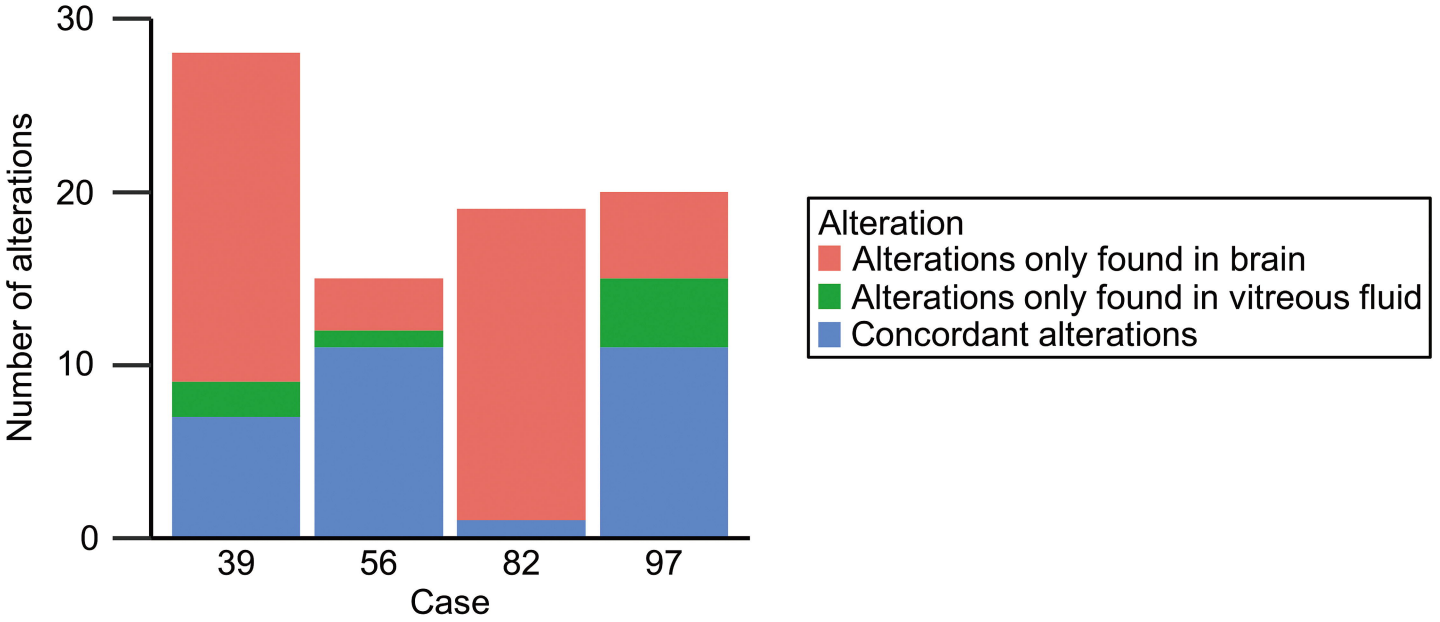

	39	56	82	97
Genetics-based CNS progression group	Intermediate	Intermediate	Slow	Rapid
Period to CNS progression	32 months	11 months	39 months	20 months

Supplementary data

Supplemental Method

Treatment for the patients

All patients underwent initial treatment with weekly intravitreal MTX injections (400 μg/100 μL) in the affected eyes until the lesions resolved. Thereafter, systemic HD-MTX (3.5 g/m2 every other week for a total of five cycles) was administered to 20/36 patients, and the remainder were carefully observed without any additional chemotherapy, according to the decision of the physician. If the treatment was not tolerated, it was discontinued at the discretion of the physician.

Flow cytometry analysis

The infiltrating cells were isolated from the vitreous humor and obtained for flow cytometry. The surface expression of B-cell markers (CD19 and CD20), T-cell markers (CD3, CD4, CD5, and CD8), and κ and λ light chains were examined. Using the criteria suggested by Levy et al.[1], we defined a monoclonal κ population as one where the κ/λ ratio was 3:1 or greater, and monoclonal λ population as one that had a λ/κ ratio in excess of 2:1.

PCR analysis of IGH rearrangement

PCR analysis of IGH rearrangement was outsourced to LSI Medience Corporation (Tokyo, Japan).

Cytokine measurement

The IL-6 and IL-10 concentrations in a vitreous humor were measured at our laboratory and SRL Corporation (Tokyo, Japan). In total, 50 μL of vitreous supernatant from each patient was used for ELISA according to the given manufacturer instructions (Invitrogen, Camarillo, CA, USA).

Amplicon-based targeted sequencing

The custom gene panel of 107 genes frequently mutated in lymphoma, and PVRL was designed using Illumina Design Studio. Covered bases were 406,093 bp, and there were 3,044 (5–157 amplicons/gene)

designed panel amplicons. This custom gene panel was designed to cover all exons of each gene on genomic DNA. As a template, 10 ng DNA amplified the target genes. Libraries were synthesized using AmpliSeq Library Plus for Illumina (Illumina, San Diego, CA, USA). The libraries were analyzed using MiSeq Reagent Kit v2 (500 cycles) with MiSeq (Illumina) platform following the provided manufacturer instructions.

Whole exome sequencing

Genomic DNA capture, enrichment, and elution were performed using Agilent SureSelect Human V6 (Agilent Technologies, Santa Clara, CA) following protocols by the manufacturer. In total, 600 ng of each genomic DNA sample was used as bait. After ligation on adaptor oligonucleotides, tail repairing, and purification, libraries were quantified by qPCR to obtain an adequate DNA template for sequencing. Synthesized libraries were sequenced on the NovaSeq 6000 (Illumina) as 150 bp pair-ended reads. Sequencing was performed by Rhelixa (Tokyo, Japan).

Gene variant discovery

Fastq files from next-generation sequencing were cleaned with Trimmomatic,[2] and the results were aligned to the human reference genome, hg19, using Burrows–Wheeler Alignment (BWA)[3]. Qualimap[4] was used to analyze coverages of mapped reads. Gene variants were detected using HaplotypeCaller included in the GATK tool[5]. Gene variants obtained from HaplotypeCaller were filtered with the parameters of quality/depth, mapping quality, and strand bias to exclude false-positive variants.[6] Variants were annotated with information from the Refseq, 1000G, and Exac databases in Illumina VariantStudio 3.0 software (Illumina). Variants with a prevalence of >1% in each regional population were excluded. COSMIC and CLINVAR databases and previous genomics research papers (Table S1) were referred to judge whether the variants were pathogenic or not.

Detection of copy number alteration

Copy number alteration for each PVRL sample were analyzed using CNVkit[7] with bam files generated by the mapping process of gene variant discovery. Consequently, the normalized coverage values of PVRL data were compared to that of uveitis cases as controls and gene copy numbers were obtained. During the

calculation process, the number of amplicons and the $\log_2$ value in control data (−5 or less) and spread of read depth (1 or more) were applied as a filter, resulting in copy number of read depth (20 or more) with low spread read depth gene regions. The $\log_2$ copy number of >0.25 was decided as gain and the $\log_2$ copy number less than −0.25 was considered as loss. CNA of *HIST1H1B*, *HIST1H1C*, *HIST1H1E*, *HIST1H4H,* and *SOCS1* were excluded from the analysis because the copy number variation between the samples was too large. In the annotation process, copy number gain of oncogene and loss of tumor suppressor gene were defined as pathogenic and incorporated into analysis. Genes with the gain of function mutations had oncogenic function were considered as oncogenes, and genes with the loss of function mutations contributed to tumorigenic pathway were considered as tumor suppressor genes (Table S1).

Table S1. Target genes included in the sequencing panel of 107 genes and the reference used for gene annotation

Gene	Mutation effect	Characteristics of mutations	Reference
ACTB	N.I.	Missense in N-terminal	Lohr et al[8], Wang et al[9]
APC	Loss of function	-	Zhang et al[10], Schmitz et al[11]
ARID1A	Loss of function	-	Zhang et al[10], Schmitz et al[11]
ARID2	Loss of function	-	Wang et al[9]
AXIN1	N.I.	-	Wang et al[9]
ATM	Loss of function	-	Schmitz et al[11]
B2M	Loss of function	-	Challa-Malladi et al[12], Schmitz et al[11]
BCL10	N.I.	-	Morin et al[13], Schmitz et al[11]
BCL2	Gain of function	-	Morin et al[13], Wang et al[9]
BCL6	N.I.	-	Morin et al[13], Schmitz et al[11]
BCL7A	Loss of function	Missense in N-terminal	Schmitz et al[11], Baliñas-Gavira et al[14]
BRCA1	Loss of function	-	Wang et al[9]
BRAF	Gain of function	Missense in hotspot (e.g. V600)	Schmitz et al[11]
BTG1	Loss of function	Missense in N-terminal	Lee et al[15], Bonzheim et al[16], Mlynarczyk et al[17]
BTG2	Loss of function	Missense in N-terminal	Lee et al[15], Bonzheim et al,[16] Wang et al[9], Mlynarczyk et al[17]
CACNA1C	N.I.	-	Lee et al[15]
BTK	Loss of function	-	Lohr et al[8], Schmitz et al[11], Hu et al[18]
CCND3	Loss of function	Missense in C-terminal hotspot	Morin et al[13], Schmitz et al[19], Schmitz et al[11]
CD274	Gain of function	-	Kataoka et al[20], Schmitz et al[11]
CD58	Loss of function	-	Challa-Malladi et al[12], Schmitz et al[11]
CD70	Loss of function	-	Schmitz et al[11]
CD79A	Gain of function	Missense in immunoreceptor tyrosine-based activation motif	Davis et al[21], Schmitz et al[11]
CD79B	Gain of function	Missense in immunoreceptor tyrosine-based activation motif (e.g. Y196)	Davis et al[21], Bonzheim et al[16], Wang et al[9]
CDKN2A	Loss of function	-	Nayyar et al[22], Wang et al[9]
CDKN2B	Loss of function	-	Nayyar et al[22], Wang et al[21]
CIITA	Loss of function	-	Mottok et al[23], Wang et al[9]
CREBBP	Loss of function	-	Bonzheim et al[16], Wang et al[9]
CSMD1	Loss of function	-	Escudero-Esparza et al[24], Lee et al[15]
CXCR4	Gain of function	Nonsense in C-terminal hotspot (e.g. S342*)	Treon et al[25], Lee et al[15]
DTX1	Loss of function	-	de Miranda et al[26], Lee et al[15]
DUSP2	N.I.	-	Lee et al[15], Wang et al[9]
EHD1	N.I.	-	Lee et al[15]
EP300	Loss of function	-	Schmitz et al[11]
ERBB4	Gain of function	-	Wang et al[9]
ETS1	Loss of function	-	Morin et al[13], Bonetti et al[27], Wang et al[9]
ETV6	Loss of function	-	Bonzheim et al[16], Wang et al[9]
EZH2	Gain of function	-	Zhang et al[10], Schmitz et al[11]
FAS	Loss of function	-	Grønbaek et al[28], Schmitz et al[11]
FAT1	Loss of function	-	Laginestra et al[29], Wang et al[9]
FAT4	Loss of function	-	Cai et al[30], Lee et al[15]
FBXW7	Loss of function	-	Wang et al[9]

FLT3	Gain of function	Missense in thymidine kinase domain (e.g. D835)	Wang et al[9]
FLT4	Gain of function	Missense in thymidine kinase domain	Liu et al[31], Wang et al[9]
FOXO1	Loss of function	Missense in phosphoinositide 3-kinase/AKT phosphorylation sites	Trinh et al[32], Wang et al[9]
FRY	Loss of function	-	Lee et al[15], Mai et al[33]
GADD45B	N.I.	-	Wang et al[9]
GNA13	Loss of function	-	Muppidi et al[34], Schmitz et al[11]
GRHPR	Loss of function	-	Lee et al[15], Andrades et al[35]
HIST1H1B	Loss of function	-	Li et al[36], Lee et al[15]
HIST1H1C	Loss of function	-	Li et al[36], Lee et al[15]
HIST1H1E	Loss of function	-	Li et al[36], Lee et al[15]
HIST1H4H	Loss of function	-	Li et al[36], Lee et al[15]
IGLL5	Loss of function	-	Bonzheim et al[16], Lee et al[15]
IKZF3	Loss of function	-	Wang et al[9]
IRF4	Loss of function	Missense in DNA binding domain	Cherian et al[37], Lee et al[15], Bonzheim et al[16], Wang et al[9]
IRF8	Loss of function	Missense in DNA binding domain	Reddy et al[38], Lee et al[15]
ITPKB	Loss of function	-	Schmitz et al[11]
KLHL14	Loss of function	-	Choi et al[39], Lee et al[15]
KLHL6	Loss of function	-	Schmitz et al[11]
KMT2D	Loss of function	-	Lee et al[15], Wang et al[9]
LRP1B	Loss of function	-	Lee et al[15]
LRIG1	N.I.	-	Lee et al[15]
MCL1	N.I.	-	Wang et al[9]
MED12	N.I.	-	Wang et al[38]
MEF2B	N.I.	-	Pon et al[40], Wang et al[9]
MALT1	N.I.	-	Schmitz et al[11]
MPEG1	Loss of function	-	Schmitz et al[11], Lee et al[15]
MUC16	N.I.	-	Lee et al[15]
MTOR	Loss of function	-	Schmitz et al[11]
MYC	Gain of function	-	Wang et al[9]
MYD88	Gain of function	-	Lee et al[15], Bonzheim et al[16], Wang et al[9]
NFKB1	Loss of function	-	Wang et al[9]
NF1	Loss of function	-	Schmitz et al[11]
NFKBIA	Loss of function	-	Schmitz et al[11], Weniger et al[41]
NFKBIE	Loss of function	-	Schmitz et al[11], Weniger et al[41]
NFKBIZ	N.I.	-	Schmitz et al[11]
NOTCH1	Gain of function	-	Schmitz et al[11]
NOTCH2	Gain of function	-	Schmitz et al[11]
OSBPL10	N.I.	-	Dobashi et al[42], Lee et al[15]
OTOF	N.I.	-	Lee et al[15]
PCDH15	N.I.	-	Lee et al[15]
PAX5	Loss of function	-	Schmitz et al[11], Gu et al[43]
PIM1	Loss of function	-	Lee et al[15], Bonzheim et al[16], Wang et al[9]
PLCG2	N.I.	-	Wang et al[9]
PRDM1	Loss of function	-	Bonzheim et al[16], Wang et al[9]
RBMX	Loss of function	-	Schmitz et al[11], Zheng et al[44]
PTEN	Loss of function	-	Schmitz et al[11]
REL	N.I.	-	Schmitz et al[11]
RP1	N.I.	-	Lee et al[15]
RUNX1	Loss of function	-	Wang et al[9]
SETBP1	Gain of function	-	Wang et al[9]

RHOA	Gain of function	-	Schmitz et al[11]
SGK1	Gain of function	-	Schmitz et al[11]
SOCS1	Loss of function	-	Schmitz et al[11]
SPEN	Loss of function	-	Reddy et al[40], Schmitz et al[11]
STAT3	Gain of function	Missense in SH2 domain (e.g. Y640F, D661Y)	Koskela et al[45], Schmitz et al[11]
STAT6	Gain of function	Missense in DNA binding domain (e.g. D419)	Yildiz et al[46], Schmitz et al[11]
TBL1XR1	Loss of function	Missense in WD domain	Venturutti et al[47], Bonzheim et al[16], Wang et al[9]
TCF3	Gain of function	-	Schmitz et al[11]
TET2	Loss of function	-	Schmitz et al[11]
TMSB4X	N.I.	-	Lee et al[15]
TNFAIP3	Loss of function	-	Kato et al[48], Schmitz et al[11]
TNFRSF14	Loss of function	-	Schmitz et al[11], Wu et al[49]
TP53	Loss of function	-	Schmitz et al[11], Wang et al[9]
UBALD2	N.I.	-	Lee et al[15]
USH2A	N.I.	-	Lee et al[15]
ZFP36L1	Loss of function	-	Reddy et al[38], Lee et al[15]

N.I., Not identified. Details of references were listed in supplementary references.

Table S2. Detected pathogenic genetic mutations

Case	Gene	Mutation type	cDNA change	AA change	VAF (%)	Read depth
1	*MYD88*	Missense	c.794T>C	p.Leu265Pro	29.36	453
1	*PIM1*	Frameshift	c.644_680delAGCCGGTGCAAGATCTCTTCGACTTCATCACGGAAAG	p.Glu215GlyfsTer138	20.99	567
1	*PIM1*	Nonsense	c.691C>T	p.Gln231Ter	40.71	565
1	*ETS1*	Nonsense	c.1323C>G	p.Tyr441Ter	27.11	439
1	*CD79B*	Missense	c.590A>G	p.Tyr197Cys	27.89	882
1	*BTG2*	Missense	c.133G>T	p.Ala45Ser	14.31	1,139
10	*TBL1XR1*	Missense	c.1108G>T	p.Asp370Tyr	55.50	582
10	*PIM1*	Splice	c.513+1G>C		57.03	619
10	*PRDM1*	Splice	c.291G>C	p.Glu97Asp	58.21	1,029
10	*PRDM1*	Splice	c.291+1G>A		58.41	1,029
10	*CDKN2A*	Missense	c.247C>T	p.His83Tyr	64.08	710
10	*ETV6*	Splice	c.33+1G>A		71.48	519
10	*CD79B*	Missense	c.590A>G	p.Tyr197Cys	78.99	2,385
10	*KLHL14*	Nonsense	c.289C>T	p.Gln97Ter	44.37	978
10	*IGLL5*	Nonsense	c.64C>T	p.Gln22Ter	42.40	500
10	*BTG2*	Missense	c.142G>A	p.Glu48Lys	43.54	2,522
10	*BTG2*	Missense	c.157C>T	p.His53Tyr	35.65	3,669
10	*BTG1*	Missense	c.498G>A	p.Met166Ile	39.23	1,300
10	*BTG1*	Missense	c.398G>A	p.Ser133Asn	44.41	1,504
10	*BTG1*	Missense	c.208A>G	p.Ile70Val	40.31	2,079
10	*BTG1*	Missense	c.129C>A	p.Ser43Arg	46.29	283
12	*MYD88*	Missense	c.794T>C	p.Leu265Pro	28.17	1,260
12	*PIM1*	Frameshift	c.149_156delGCAACGCC	p.Arg50HisfsTer13	56.27	670
12	*PIM1*	Frameshift	c.276delG	p.Met92IlefsTer93	60.48	625
12	*PIM1*	Nonsense	c.676G>T	p.Glu226Ter	48.71	1,944
12	*PIM1*	Nonsense	c.720_748delGCAGGTGCTGGAGGCCGTGCGGCACTGCC	p.Trp240Ter	24.73	1,326
12	*PRDM1*	Frameshift	c.500_522delCTCCCCGGGAGCAAAACCTGGCT	p.Ser167CysfsTer14	34.95	495
12	*ACTB*	Missense	c.143G>A	p.Gly48Asp	26.49	1,797
12	*ETV6*	Nonsense	c.19C>T	p.Gln7Ter	30.12	601
12	*ETV6*	Missense	c.1172A>G	p.Tyr391Cys	23.27	709
12	*BTG1*	Nonsense	c.103C>T	p.Arg35Ter	37.11	256

12	*KLHL14*	Frameshift	c.625_635delCTGGTGGAGGA	p.Leu209CysfsTer47	34.28	878
12	*KLHL14*	Nonsense	c.271C>T	p.Gln91Ter	29.34	634
12	*IGLL5*	Splice	c.206+2T>A		24.32	6,187
12	*BTG2*	Missense	c.83G>A	p.Gly28Asp	26.39	2,876
12	*BTG2*	Missense	c.185G>C	p.Gly62Ala	25.24	2,524
12	*BTG1*	Missense	c.304C>T	p.Leu102Phe	31.11	270
12	*BTG1*	Missense	c.116C>T	p.Thr39Ile	36.33	256
22	*MYD88*	Missense	c.794T>C	p.Leu265Pro	31.92	639
22	*TBL1XR1*	Missense	c.941T>A	p.Val314Asp	37.48	643
22	*HIST1H1B*	Missense	c.392C>G	p.Ala131Gly	73.16	395
22	*PIM1*	Nonsense	c.652C>T	p.Gln218Ter	48.17	546
22	*PRDM1*	Splice	c.291G>C	p.Glu97Asp	74.72	542
22	*CDKN2A*	Missense	c.197A>G	p.His66Arg	85.45	55
22	*PTEN*	Frameshift	c.149_153dupTTGAT	p.Asp52LeufsTer4	27.35	1,104
22	*MPEG1*	Nonsense	c.271C>T	p.Gln91Ter	33.27	505
22	*KMT2D*	Nonsense	c.6229C>T	p.Gln2077Ter	38.25	1,336
22	*CIITA*	Nonsense	c.657C>A	p.Cys219Ter	36.02	1,180
22	*CD79B*	Missense	c.590A>C	p.Tyr197Ser	34.73	976
26	*BTG2*	Nonsense	c.16G>T	p.Gly6Ter	47.99	2,761
26	*MYD88*	Missense	c.794T>C	p.Leu265Pro	39.86	1,041
26	*TBL1XR1*	Missense	c.1099T>C	p.Cys367Arg	38.34	866
26	*HIST1H1B*	Frameshift	c.230_257delAGAAGAATAACAGCCGCATTAAGCTGGG	p.Glu77AlafsTer6	18.61	1,752
26	*PIM1*	Nonsense	c.387C>G	p.Tyr129Ter	51.70	853
26	*PAX5*	Splice	c.41_46+13delGGACAGGTAGGACCGCGAT		35.36	1,151
26	*GRHPR*	Frameshift	c.129_130delGG	p.Glu44AlafsTer48	15.02	486
26	*GRHPR*	Frameshift	c.129_130delGG	p.Glu44AlafsTer48	15.02	486
26	*GRHPR*	Frameshift	c.129_130delGG	p.Glu44AlafsTer48	15.02	486
26	*MPEG1*	Nonsense	c.1201G>T	p.Glu401Ter	29.63	1,441
26	*MPEG1*	Frameshift	c.1195_1196delAA	p.Lys399ValfsTer10	36.38	1,443
26	*MPEG1*	Frameshift	c.920delG	p.Gly307AlafsTer21	29.60	1,108
26	*ETV6*	Splice	c.33+1G>C		57.42	404
26	*ETV6*	Nonsense	c.427C>T	p.Gln143Ter	54.02	1,405
26	*KMT2D*	Nonsense	c.14152G>T	p.Glu4718Ter	43.40	1,719
26	*CIITA*	Nonsense	c.1099C>T	p.Gln367Ter	30.15	617
26	*CIITA*	Frameshift	c.3052delG	p.Glu1018LysfsTer32	62.17	423

26	*BCL2*	Missense	c.351C>G	p.Ser117Arg	24.56	2,895
26	*BCL2*	Missense	c.20C>T	p.Thr7Ile	27.50	1,491
26	*GRHPR*	Frameshift	c.129_130delGG	p.Glu44AlafsTer48	15.02	486
26	*GRHPR*	Frameshift	c.129_130delGG	p.Glu44AlafsTer48	15.02	486
26	*BTG2*	Missense	c.96G>T	p.Glu32Asp	26.12	2,726
31	*MYD88*	Missense	c.794T>C	p.Leu265Pro	34.50	774
31	*TBL1XR1*	Missense	c.1051G>A	p.Glu351Lys	32.16	398
31	*TET2*	Frameshift	c.4745_4746delCT	p.Ser1582PhefsTer31	12.00	175
31	*PIM1*	Frameshift	c.201_214delGCACAGCCCCGGCT	p.His68ArgfsTer101	73.88	157
31	*PIM1*	Splice	c.513+1G>A		30.50	400
31	*PIM1*	Nonsense	c.652C>T	p.Gln218Ter	56.61	295
31	*PIM1*	Nonsense	c.691C>T	p.Gln231Ter	33.74	492
31	*PIM1*	Frameshift	c.711_724delCTTCTTCTGGCAGG	p.Phe238AlafsTer57	38.14	527
31	*PIM1*	Nonsense	c.1057G>T	p.Glu353Ter	24.67	608
31	*ETV6*	Splice	c.34-1G>A		29.54	799
31	*ETV6*	Splice	c.1254-2A>G		31.91	564
31	*KMT2D*	Nonsense	c.11911C>T	p.Gln3971Ter	33.17	612
31	*DTX1*	Nonsense	c.229C>T	p.Gln77Ter	32.22	239
31	*CD79B*	Missense	c.589T>C	p.Tyr197His	69.73	621
31	*BTG1*	Missense	c.347G>A	p.Gly116Glu	41.59	428
31	*BTG1*	Missense	c.145G>A	p.Ala49Thr	36.11	144
39	*MYD88*	Missense	c.794T>C	p.Leu265Pro	39.48	423
39	*KMT2D*	Nonsense	c.12844C>T	p.Arg4282Ter	34.29	35
49	*MYD88*	Missense	c.794T>C	p.Leu265Pro	46.60	515
49	*PIM1*	Nonsense	c.697G>T	p.Glu233Ter	73.22	956
49	*PIM1*	Frameshift	c.737_740delTGCG	p.Val246GlyfsTer118	73.17	954
49	*CD79B*	Missense	c.590A>C	p.Tyr197Ser	48.21	1,931
49	*KLHL14*	Nonsense	c.763C>T	p.Gln255Ter	47.42	1,242
49	*KLHL14*	Nonsense	c.735G>A	p.Trp245Ter	42.69	1,225
49	*BTG1*	Missense	c.123C>G	p.Ser41Arg	42.96	135
49	*BTG1*	Missense	c.108G>C	p.Gln36His	42.96	135
52	*PIM1*	Nonsense	c.927C>G	p.Tyr309Ter	33.15	374
52	*PRDM1*	Nonsense	c.232C>T	p.Gln78Ter	50.64	543
52	*ACTB*	Missense	c.217C>T	p.His73Tyr	68.18	396
52	*CSMD1*	Nonsense	c.9254G>A	p.Trp3085Ter	30.49	505
52	*ETV6*	Missense	c.1256T>G	p.Phe419Cys	33.62	687
52	*BCL7A*	Missense	c.91T>C	p.Trp31Arg	32.85	137

52	*CREBBP*	Missense	c.4463C>T	p.Pro1488Leu	48.61	1,473
52	*CD79B*	Missense	c.590A>G	p.Tyr197Cys	58.42	1,152
52	*MYD88*	Missense	c.794T>C	p.Leu265Pro	63.94	391
52	*BTG2*	Missense	c.273G>C	p.Gln91His	42.53	783
56	*PIM1*	Nonsense	c.382C>T	p.Gln128Ter	55.11	303
56	*ACTB*	Missense	c.137G>C	p.Gly46Ala	33.64	431
56	*CD79B*	Missense	c.590A>C	p.Tyr197Ser	34.32	1,110
56	*MYD88*	Missense	c.794T>C	p.Leu265Pro	43.04	381
56	*BTG1*	Nonsense	c.168G>A	p.Trp56Ter	57.03	626
56	*BTG1*	Missense	c.400A>T	p.Thr134Ser	50.12	431
56	*BTG1*	Missense	c.160C>T	p.His54Tyr	57.03	626
56	*BTG1*	Missense	c.8C>T	p.Pro3Leu	26.63	612
61	*PIM1*	Nonsense	c.387C>A	p.Tyr129Ter	48.55	1,584
61	*PIM1*	Splice	c.513+1G>A		38.99	418
61	*KMT2D*	Splice	c.10441-2A>G		66.88	2,962
61	*IKZF3*	Splice	c.826+1G>T		52.79	1,847
61	*BTG2*	Frameshift	c.100_124delAGGCTTAAGGTCTTCAGCGGGGCGC	p.Arg34SerfsTer59	41.52	2,271
61	*MYD88*	Missense	c.794T>C	p.Leu265Pro	94.93	592
61	*BTG1*	Missense	c.14A>T	p.Tyr5Phe	20.82	1,047
82	*SOCS1*	Frameshift	c.312_330delCGACAGCCGCCAGCGGAAC	p.Asp105AlafsTer7	23.05	564
87	*LRP1B*	Splice	c.1971-2A>T		47.28	1,303
87	*TBL1XR1*	Missense	c.920A>G	p.His307Arg	50.79	1,262
87	*BCL7A*	Splice	c.92+1G>A		41.35	237
87	*CREBBP*	Nonsense	c.5701C>T	p.Gln1901Ter	50.00	92
87	*NF1*	Nonsense	c.669G>A	p.Trp223Ter	45.19	135
87	*BTG2*	Missense	c.52G>A	p.Gly18Ser	53.98	2,321
87	*BTG2*	Missense	c.83G>A	p.Gly28Asp	53.83	2,326
87	*BTG2*	Missense	c.133G>T	p.Ala45Ser	53.64	2,321
87	*BTG2*	Missense	c.136C>T	p.Leu46Phe	40.55	2,328
97	*PIM1*	Nonsense	c.652C>T	p.Gln218Ter	80.38	581
97	*PIM1*	Nonsense	c.720G>A	p.Trp240Ter	41.68	715
97	*PIM1*	Nonsense	c.908G>A	p.Trp303Ter	41.99	443
97	*PRDM1*	Splice	c.291G>C	p.Glu97Asp	51.92	728
97	*GRHPR*	Splice	c.214+1G>A		41.75	103
97	*GRHPR*	Splice	c.287+1G>A		36.71	779
97	*KMT2D*	Frameshift	c.15891_15895dupGGTGC	p.His5299ArgfsTer8	37.80	463

97	*CD79B*	Missense	c.590A>G	p.Tyr197Cys	33.35	1,475
97	*BTG2*	Splice	c.142+1G>C		30.43	1,620
97	*MYD88*	Missense	c.794T>C	p.Leu265Pro	33.06	605
97	*MPEG1*	Nonsense	c.556C>T	p.Gln186Ter	29.55	714
114	*FBXW7*	Missense	c.1513C>T	p.Arg505Cys	47.07	2,422
114	*IRF4*	Missense	c.208C>G	p.Leu70Val	26.67	30
114	*PIM1*	Frameshift	c.245_249delGTCCC	p.Arg82LeufsTer90	60.07	263
114	*PIM1*	Frameshift	c.674_702delCGGAAAGGGGAGCCCTGCAAGAGGAGCTG	p.Thr225SerfsTer65	84.02	795
114	*CSMD1*	Splice	c.9814+1G>A		44.04	965
114	*ETV6*	Splice	c.12_33+24delTCCTGCTCAGTGTAGCATTAAGGTAAAAATCTTCTCCCCTCCTTCT		50.84	356
114	*BCL7A*	Missense	c.70G>A	p.Ala24Thr	46.23	106
114	*KLHL14*	Nonsense	c.562C>T	p.Gln188Ter	33.91	929
114	*KLHL14*	Nonsense	c.550C>T	p.Gln184Ter	42.80	736
114	*MYD88*	Missense	c.794T>C	p.Leu265Pro	45.77	627
114	*MEF2B*	Frameshift	c.396_399dupTGCA	p.Ala134CysfsTer21	46.81	94
114	*BTG2*	Missense	c.83G>A	p.Gly28Asp	32.40	1,923
114	*BTG2*	Missense	c.92G>A	p.Ser31Asn	32.40	1,923
126	*FAT4*	Nonsense	c.3754G>T	p.Gly1252Ter	36.60	806
126	*FRY*	Frameshift	c.2667delT	p.Leu890TrpfsTer30	20.41	49
132	*ITPKB*	Nonsense	c.691A>T	p.Lys231Ter	32.56	1,170
132	*MYD88*	Missense	c.794T>C	p.Leu265Pro	54.79	1,608
132	*TBL1XR1*	Missense	c.1184A>T	p.Tyr395Phe	44.29	736
132	*ACTB*	Missense	c.193C>T	p.Leu65Phe	28.15	959
132	*GRHPR*	Splice	c.214+1G>A		43.33	90
132	*ETV6*	Splice	c.33+1G>A		54.30	151
132	*IRF8*	Missense	c.197A>G	p.Lys66Arg	38.90	365
132	*BTG2*	Missense	c.83G>A	p.Gly28Asp	29.77	2,267
136	*MYD88*	Missense	c.794T>C	p.Leu265Pro	64.93	211
136	*HIST1H1E*	Missense	c.308G>A	p.Gly103Asp	22.31	130
136	*IGLL5*	Frameshift	c.32_41delAGACCCCTGA	p.Glu11GlyfsTer95	33.33	75
136	*RBMX*	Frameshift	c.1dupA	p.Met1?	36.17	47
136	*KMT2D*	Nonsense	c.2635G>T	p.Glu879Ter	38.58	127
136	*BCL7A*	Nonsense	c.92G>A	p.Trp31Ter	28.57	77
137	*CD58*	Nonsense	c.471C>G	p.Tyr157Ter	35.48	1,581
137	*CD58*	Nonsense	c.454C>T	p.Arg152Ter	38.45	1,597

137	*ITPKB*	Nonsense	c.622C>T	p.Gln208Ter	30.72	345
137	*MYD88*	Missense	c.794T>C	p.Leu265Pro	36.47	987
137	*TBL1XR1*	Missense	c.1200T>A	p.Ser400Arg	37.32	142
137	*TBL1XR1*	Missense	c.1124T>A	p.Ile375Lys	40.46	131
137	*TBL1XR1*	Missense	c.1123A>G	p.Ile375Val	40.46	131
137	*PIM1*	Nonsense	c.481G>T	p.Glu161Ter	38.11	677
137	*CDKN2A*	Nonsense	c.330G>A	p.Trp110Ter	36.89	862
137	*BCL7A*	Missense	c.86G>A	p.Arg29His	31.16	276
137	*CIITA*	Frameshift	c.3021delC	p.Ser1008GlnfsTer7	39.45	512
137	*CD79B*	Missense	c.589T>G	p.Tyr197Asp	34.08	1,247
137	*GNA13*	Nonsense	c.79C>T	p.Gln27Ter	27.96	651
139	*MYD88*	Missense	c.794T>C	p.Leu265Pro	54.98	1,346
139	*PIM1*	Nonsense	c.361G>T	p.Glu121Ter	39.10	693
139	*PRDM1*	Frameshift	c.485_486delTG	p.Val162GlufsTer26	81.73	197
139	*ETV6*	Splice	c.33+1G>C		83.65	159
139	*CREBBP*	Missense	c.4472A>C	p.Gln1491Pro	43.25	1,519
139	*TP53*	Missense	c.761T>A	p.Ile254Asn	82.95	733
139	*CD79B*	Missense	c.589T>G	p.Tyr197Asp	45.48	1,172
139	*IGLL5*	Frameshift	c.93_94delGG	p.Ala32HisfsTer59	91.19	590
139	*BTG1*	Missense	c.116C>T	p.Thr39Ile	46.44	239
144	*MYD88*	Missense	c.794T>C	p.Leu265Pro	34.62	1,352
144	*PRDM1*	Splice	c.291G>C	p.Glu97Asp	53.34	718
144	*CD79B*	Missense	c.590A>G	p.Tyr197Cys	32.83	1,185
144	*KLHL14*	Nonsense	c.289C>T	p.Gln97Ter	38.02	313
144	*BTG1*	Missense	c.17C>T	p.Thr6Ile	33.89	773
147	*GRHPR*	Splice	c.287+1G>A		22.31	1,013
147	*ETV6*	Splice	c.33+1delG		20.29	138
147	*IGLL5*	Frameshift	c.212delT	p.Leu71ArgfsTer38	31.77	1,432
147	*MYD88*	Missense	c.794T>C	p.Leu265Pro	31.90	1,279
147	*MPEG1*	Nonsense	c.2131C>T	p.Gln711Ter	17.74	248
173	*CSMD1*	Nonsense	c.585G>A	p.Trp195Ter	42.10	38
174	*MYD88*	Missense	c.794T>C	p.Leu265Pro	21.72	1,625
174	*TBL1XR1*	Missense	c.1100G>C	p.Cys367Ser	23.48	1,001
174	*PRDM1*	Splice	c.291G>A	c.291G>A(p.=)	27.79	662
174	*PRDM1*	Splice	c.291+1G>A		27.79	662
174	*CDKN2A*	Nonsense	c.329G>A	p.Trp110Ter	49.78	1,137
174	*KMT2D*	Nonsense	c.8050C>T	p.Gln2684Ter	25.77	2,716

174	*ZFP36L1*	Nonsense	c.567C>A	p.Cys189Ter	27.47	1,791
174	*KLHL14*	Nonsense	c.562C>T	p.Gln188Ter	35.16	2,076
179	*NOTCH2*	Nonsense	c.7090C>T	p.Gln2364Ter	55.59	1,423
179	*BTG2*	Frameshift	c.115_116insACTTAAGGTCTTCA	p.Ser39AsnfsTer67	29.44	1,155
179	*BTG2*	Frameshift	c.115_116insATTTAAGGTCTTCA	p.Ser39AsnfsTer67	20.61	1,155
179	*CD79B*	Missense	c.590A>C	p.Tyr197Ser	94.96	873
179	*GNA13*	Nonsense	c.111C>A	p.Cys37Ter	42.96	568
179	*BTG2*	Missense	c.83G>A	p.Gly28Asp	40.72	1,159
179	*BTG2*	Missense	c.121G>C	p.Ala41Pro	40.40	1,161
180	*MYD88*	Missense	c.794T>C	p.Leu265Pro	42.18	211
180	*IRF4*	Nonsense	c.178C>T	p.Gln60Ter	34.41	186
180	*IRF4*	Missense	c.208C>G	p.Leu70Val	94.69	113
180	*CD79B*	Missense	c.589T>G	p.Tyr197Asp	59.78	184
180	*KMT2D*	Nonsense	c.12253C>T	p.Gln4085Ter	42.86	252
180	*PIM1*	Splice	c.355+1G>C		96.80	437
180	*ETV6*	Splice	c.33+1G>C		54.95	202
180	*ETV6*	Splice	c.33+1delG		37.62	202
182	*GNA13*	Splice	c.283+1G>A		25.63	355
184	*MYD88*	Missense	c.794T>C	p.Leu265Pro	38.05	1,201
184	*TBL1XR1*	Missense	c.971C>T	p.Ser324Phe	78.37	1,946
184	*PIM1*	Splice	c.355+1G>A		39.38	678
184	*PIM1*	Nonsense	c.432C>A	p.Tyr144Ter	66.80	253
184	*PIM1*	Frameshift	c.704_711delCCCGCAGC	p.Ala235ValfsTer62	23.55	1,622
184	*GRHPR*	Splice	c.215-9_217delGCACAACAGGGG		44.26	1,803
184	*GRHPR*	Frameshift	c.220_221delAA	p.Asn74SerfsTer18	44.36	1,799
184	*MPEG1*	Nonsense	c.1687C>T	p.Gln563Ter	39.23	989
184	*ETV6*	Splice	c.31_33+8delAAGGTAAAAAT		80.45	133
184	*ZFP36L1*	Frameshift	c.750delG	p.Glu250AspfsTer52	29.03	31
184	*IGLL5*	Frameshift	c.158_179delGAGCCTCAGTTGGAAGCAGCCG	p.Gly53AspfsTer49	62.22	532
184	*BTG2*	Missense	c.20C>T	p.Thr7Ile	59.84	1,367
184	*BTG2*	Missense	c.277C>T	p.His93Tyr	37.53	1,327
184	*BTG1*	Missense	c.197G>A	p.Gly66Asp	43.70	540
184	*BTG1*	Missense	c.108G>C	p.Gln36His	39.51	205
184	*BTG1*	Missense	c.91C>T	p.Leu31Phe	40.10	207

189	*MYD88*	Missense	c.794T>C	p.Leu265Pro	88.47	1,102
189	*CD79A*	Nonsense	c.553G>T	p.Glu185Ter	52.75	728
189	*IGLL5*	Splice	c.206+1G>T		35.00	3,177
197	*FBXW7*	Missense	c.1393C>T	p.Arg465Cys	24.71	603
197	*CD79B*	Missense	c.589T>A	p.Tyr197Asn	28.35	1,252
197	*EP300*	Splice	c.1529-2A>T		33.33	222
204	*HIST1H1C*	Frameshift	c.199_200delGC	p.Ala67CysfsTer5	40.15	259
204	*IRF8*	Missense	c.67T>C	p.Tyr23His	45.67	1,743
204	*CD79B*	Missense	c.590A>C	p.Tyr197Ser	38.41	2,114
204	*GNA13*	Frameshift	c.93delC	p.Lys32ArgfsTer14	39.48	1,145
204	*GNA13*	Frameshift	c.80_89delAGCAACGCAA	p.Gln27ArgfsTer16	39.60	1,149
204	*IGLL5*	Splice	c.206+17_206+18insTCAGGTAAGGGGCAAGAGATT		49.00	1,945
204	*MYD88*	Missense	c.794T>C	p.Leu265Pro	46.65	701
204	*BTG1*	Missense	c.206G>A	p.Cys69Tyr	27.07	1,330

Abbreviations: AA, amino acid; VAF, variant allele frequency

Table S3. Detected pathogenic copy number alterations

Case	Gene	CNA	Log_2	Case	Gene	CNA	Log_2	Case	Gene	CNA	Log_2
1	*CDKN2A*	Loss	−0.91	**49**	*BCL2*	Gain	0.78	**139**	*FLT3*	Gain	0.45
1	*CDKN2B*	Loss	−0.64	**49**	*CD58*	Loss	−0.28	**139**	*PRDM1*	Loss	−0.75
1	*CSMD1*	Loss	−0.51	**49**	*CDKN2A*	Loss	−3.17	**139**	*SGK1*	Loss	−0.89
1	*IGLL5*	Loss	−0.45	**49**	*CDKN2B*	Loss	−4.32	**139**	*TNFAIP3*	Loss	−0.94
1	*MYC*	Gain	0.53	**49**	*CIITA*	Loss	−0.74	**139**	*TP53*	Loss	−0.82
1	*PRDM1*	Loss	−0.37	**49**	*ETV6*	Loss	−0.95	**144**	*CDKN2A*	Loss	−1.12
1	*SGK1*	Loss	−0.47	**49**	*IGLL5*	Loss	−3.46	**144**	*CDKN2B*	Loss	−1.68
1	*TNFAIP3*	Loss	−0.52	**49**	*MALT1*	Gain	0.78	**144**	*PRDM1*	Loss	−0.53
10	*BCL7A*	Loss	−0.45	**52**	*CDKN2A*	Loss	−1.28	**144**	*SGK1*	Loss	−0.36
10	*CDKN2A*	Loss	−0.68	**52**	*CDKN2B*	Loss	−2.51	**144**	*STAT6*	Gain	0.80
10	*CDKN2B*	Loss	−1.29	**52**	*MEF2B*	Loss	−0.61	**144**	*TNFAIP3*	Loss	−0.55
10	*ETV6*	Loss	−0.54	**56**	*CDKN2A*	Loss	−2.61	**179**	*STAT6*	Gain	0.83
10	*KMT2D*	Loss	−0.65	**56**	*CDKN2B*	Loss	−3.49	**179**	*CDKN2A*	Loss	−3.74
10	*PRDM1*	Loss	−1.30	**56**	*PRDM1*	Loss	−2.36	**179**	*CDKN2B*	Loss	−3.79
12	*CDKN2A*	Loss	−0.78	**61**	*BCL7A*	Loss	−0.56	**180**	*BCL2*	Gain	0.87
12	*CDKN2B*	Loss	−0.84	**61**	*CDKN2A*	Loss	−3.11	**180**	*BCL7A*	Loss	−0.69
12	*IGLL5*	Loss	−0.49	**61**	*CDKN2B*	Loss	−2.27	**180**	*CD274*	Gain	0.74
12	*PIM1*	Loss	−0.55	**61**	*IGLL5*	Loss	−1.43	**180**	*CDKN2A*	Loss	−3.09
12	*PRDM1*	Loss	−0.36	**61**	*PRDM1*	Loss	−0.92	**180**	*CDKN2B*	Loss	−1.34
12	*SGK1*	Loss	−0.33	**61**	*SGK1*	Loss	−0.70	**180**	*MALT1*	Gain	0.55
12	*TNFAIP3*	Loss	−0.37	**61**	*TNFAIP3*	Loss	−0.90	**180**	*SETBP1*	Gain	0.69
22	*CDKN2A*	Loss	−2.48	**87**	*CDKN2A*	Loss	−4.01	**184**	*ARID2*	Loss	−0.75
22	*CDKN2B*	Loss	−2.33	**87**	*CDKN2B*	Loss	−4.51	**184**	*CDKN2A*	Loss	−2.52
22	*CSMD1*	Loss	−0.76	**97**	*CDKN2A*	Loss	−3.14	**184**	*CDKN2B*	Loss	−2.35
22	*ETV6*	Loss	−0.68	**97**	*CDKN2B*	Loss	−1.54	**184**	*CSMD1*	Loss	−0.61
22	*IGLL5*	Loss	−2.77	**97**	*ETV6*	Loss	−1.54	**184**	*ETV6*	Loss	−0.51
22	*MEF2B*	Loss	−0.52	**97**	*NFKBIZ*	Gain	0.47	**184**	*PRDM1*	Loss	−0.82
22	*PRDM1*	Loss	−0.81	**114**	*CDKN2A*	Loss	−1.05	**184**	*SGK1*	Loss	−1.10
26	*CDKN2A*	Loss	−0.32	**114**	*CDKN2B*	Loss	−1.66	**184**	*TNFAIP3*	Loss	−0.81
26	*ETV6*	Loss	−0.42	**114**	*MPEG1*	Loss	−0.78	**189**	*MCL1*	Gain	0.81
26	*IGLL5*	Loss	−1.69	**132**	*CDKN2A*	Loss	−1.90	**189**	*BRAF*	Gain	0.38
26	*MALT1*	Gain	0.60	**132**	*CDKN2B*	Loss	−1.75	**189**	*STAT6*	Gain	0.38

26	*SETBP1*	Gain	0.56	**132**	*NFKBIZ*	Gain	0.50	**189**	*PRDM1*	Loss	−0.75
31	*BCL2*	Gain	0.48	**132**	*RHOA*	Gain	0.81	**189**	*SGK1*	Loss	−0.71
31	*CDKN2A*	Loss	−1.46	**132**	*SGK1*	Loss	−0.71	**189**	*TNFAIP3*	Loss	−0.72
31	*CDKN2B*	Loss	−1.67	**132**	*TNFAIP3*	Loss	−0.91	**197**	*STAT6*	Gain	0.63
31	*MALT1*	Gain	0.51	**136**	*CDKN2A*	Loss	−0.83	**197**	*CDKN2A*	Loss	−1.04
31	*PRDM1*	Loss	−0.56	**136**	*CDKN2B*	Loss	−0.85	**197**	*IGLL5*	Loss	−1.11
31	*SETBP1*	Gain	0.53	**136**	*PRDM1*	Loss	−0.50	**204**	*CDKN2A*	Loss	−4.93
31	*TMSB4X*	Gain	0.96	**136**	*SGK1*	Loss	−0.79	**204**	*CDKN2B*	Loss	−2.11
39	*CD274*	Gain	0.68	**136**	*TNFAIP3*	Loss	−0.38	**204**	*CREBBP*	Loss	−0.80
39	*CDKN2A*	Loss	−3.86	**137**	*SGK1*	Loss	−0.79	**204**	*IGLL5*	Loss	−1.19
39	*CDKN2B*	Loss	−4.63	**139**	*CDKN2A*	Loss	−2.85	**204**	*PRDM1*	Loss	−0.90
39	*ETV6*	Loss	−2.81	**139**	*CDKN2B*	Loss	−3.62	**204**	*SGK1*	Loss	−0.93
39	*IGLL5*	Loss	−0.86	**139**	*ETV6*	Loss	−0.57	**204**	*TNFAIP3*	Loss	−1.11

Abbreviations: CNA, copy number alteration

Table S4. Relationship between *ETV6* loss and clinical findings

Factors	*ETV6* loss		p-value
	Positive (n = 8)	Negative (n = 27)	
Sex, male/female	3/5	11/16	1
Age, median (range), years	71.5 (45–83)	69 (43–84)	0.70
Laterality, unilateral/bilateral	3/5	12/15	1
IL-10 level (pg/mL), median (range)	890 (17–5005)	1008 (10-130,125)	0.50
IL-10/IL-6 ratio	12.6 (0.29–98.1)	15.6 (0.46–1161.8)	0.26
Cytopathology positive (class ≥IIIb)	6/2	17/10	0.69
Detection of B-cell clonality (FCM analysis)	5/1	18/6	1
Positive for *IGH* rearrangement (PCR)	8/0	20/6	0.30
WBC (/μL), median (range)	5950 (4500–13,000)	6200 (3600–12,400)	0.84
ANC (/μL), median (range)	3735 (2547–10,946)	4018 (2051–11,284)	0.95
ALC (/μL), median (range)	1905 (1363–2539)	1488 (792–3834)	0.24
LDH (U/L), median (range)	220.5 (163–376)	199 (141–274)	0.38
sIL-2R (U/mL), median (range)	269.5 (208.4–4040)	321 (107–762)	0.40
CRP (mg/dL), median (range)	0.06 (0.02–0.48)	0.05 (0.02–0.54)	0.41

p-values < 0.05 were considered statistically significant.

Abbreviations: ALC, absolute lymphocyte count; ANC, absolute neutrophil count; CRP, C-reactive protein; FCM, flow cytometry; IL, interleukin; LDH, lactate dehydrogenase; PCR, polymerase chain reaction; sIL-2R, soluble interleukin-2 receptor, WBC, white blood cell

Table S5. Relationship between *PRDM1* alteration and clinical findings

Factors	*PRDM1* alteration		p-value
	Positive (n = 17)	Negative (n = 18)	
Sex, male/female	9/8	5/13	0.18
Age, median (range), years	72 (45–83)	69.5 (43–84)	0.47
Laterality, unilateral/bilateral	5/12	10/8	0.18
IL-10 level (pg/mL), median (range)	738 (137–130,125)	1192 (10–10,596)	0.64
IL-10/IL-6 ratio	17.4 (1.2–1161.8)	13.0 (0.29–190.6)	0.22
Cytopathology positive (class ≥IIIb)	12/5	11/7	0.73
B-cell clonality (FCM analysis)	11/4	12/3	1
Positive for *IGH* gene rearrangement (PCR)	12/4	16/2	0.39
WBC (/μL), median (range)	6000 (4100–13000)	6200 (3600–12,400)	0.87
ANC (/μL), median (range)	3870 (2378–10946)	3959 (2051–11,284)	0.88
ALC (/μL), median (range)	1488 (968–2539)	1632.5 (792–3834)	0.82
LDH (U/L), median (range)	199 (157–376)	212.5 (141–274)	0.88
sIL-2R (U/mL), median (range)	287.1 (125–4040)	341.5 (107–762)	0.31
CRP (mg/dL), median (range)	0.04 (0.02–0.48)	0.065 (0.02–0.54)	0.69

p-values < 0.05 were considered statistically significant.

Abbreviations: ALC, absolute lymphocyte count; ANC, absolute neutrophil count; CRP, C-reactive protein; FCM, flow cytometry; IL, interleukin; LDH, lactate dehydrogenase; PCR, polymerase chain reaction; sIL-2R, soluble interleukin-2 receptor; WBC, white blood cell

Table S6. Pathogenic gene alteration in primary vitreoretinal lymphoma patients with central nervous system progression

	Vitreous humor					Brain				
Case	**Gene**	**Mutation type**	**cDNA change**	**AA change**	**VAF**	**Gene**	**Mutation type**	**cDNA change**	**AA change**	**VAF**
39	*MYD88*	Missense	c.794T>C	p.Leu265Pro	39.48	*MYD88*	Missense	c.794T>C	p.Leu265Pro	90.42
	KMT2D	Nonsense	c.12844C>T	p.Arg4282Ter	34.29	*KMT2D*	Nonsense	c.12844C>T	p.Arg4282Ter	70.33
	CD274	Gain				*CD274*	Gain			
	CDKN2A	Loss				*CDKN2A*	Loss			
	CDKN2B	Loss				*CDKN2B*	Loss			
	IGLL5	Loss				*IGLL5*	Loss			
	ETV6	Loss				-				
	-					*ACTB*	Gain			
	-					*CD58*	Frameshift	c.218delC	p.Ala73ValfsTer11	91.62
	-					*IRF4*	Missense	c.170C>T	p.Ala57Val	64.48
	-					*HIST1H1C*	Missense	c.347C>G	p.Ala116Gly	94.51
	-					*HIST1H4H*	Missense	c.28G>T	p.Gly10Cys	34.31
	-					*MYC*	Missense	c.63C>G	p.Ser21Arg	63.02
	-					*MYC*	Missense	c.106C>T	p.Pro36Ser	63.35
	-					*MYC*	Missense	c.650G>C	p.Ser217Thr	62.87
	-					*CD79B*	Missense	c.589T>C	p.Tyr197His	57.61
	-					*BRAF*	Gain			
	-					*STAT6*	Gain			
	-					*B2M*	Loss			
56	*ACTB*	Missense	c.137G>C	p.Gly46Ala	33.64	*ACTB*	Missense	c.137G>C	p.Gly46Ala	40.37
	CD79B	Missense	c.590A>C	p.Tyr197Ser	34.32	*CD79B*	Missense	c.590A>C	p.Tyr197Ser	39.56
	MYD88	Missense	c.794T>C	p.Leu265Pro	43.04	*MYD88*	Missense	c.794T>C	p.Leu265Pro	40.16
	BTG1	Missense	c.400A>T	p.Thr134Ser	50.12	*BTG1*	Missense	c.400A>T	p.Thr134Ser	39.05
	BTG1	Missense	c.160C>T	p.His54Tyr	57.03	*BTG1*	Missense	c.160C>T	p.His54Tyr	38.59
	BTG1	Nonsense	c.168G>A	p.Trp56Ter	57.03	*BTG1*	Nonsense	c.168G>A	p.Trp56Ter	38.59
	BTG1	Missense	c.8C>T	p.Pro3Leu	26.63	*BTG1*	Missense	c.8C>T	p.Pro3Leu	35.94
	PRDM1	Loss				*PRDM1*	Loss			
	CDKN2A	Loss				*CDKN2A*	Loss			
	CDKN2B	Loss				*CDKN2B*	Loss			
	PIM1	Nonsense	c.382C>T	p.Gln128Ter	55.11	-				

	KMT2D	Loss				-				
	BCL7A	Loss				-				
	-					*BTG1*	Missense	c.316G>A	p.Val106Ile	42.37
	-					*GNA13*	Nonsense	c.79C>T	p.Gln27Ter	41.29
82	*SOCS1*	Frameshift	c.312_330delCGACAGCCGCCAGCGGAAC	p.Asp105AlafsTer7	23.05	*SOCS1*	Frameshift	c.312_330delCGACAGCCGCCAGCGGAAC	p.Asp105AlafsTer7	49.62
	-					*MYD88*	Gain			
	-					*RHOA*	Gain			
	-					*TET2*	Loss			
	-					*FAT4*	Loss			
	-					*FBXW7*	Loss			
	-					*FAT1*	Loss			
	-					*CDKN2A*	Loss			
	-					*CDKN2B*	Loss			
	-					*IGLL5*	Loss			
	-					*MYD88*	Missense	c.794T>C	p.Leu265Pro	42.32
	-					*HIST1H1E*	Missense	c.536C>T	p.Ala179Val	24.25
	-					*PIM1*	Splice	c.356-1G>A		40.08
	-					*PRDM1*	Nonsense	c.1230C>A	p.Tyr410Ter	78.49
	-					*ACTB*	Missense	c.585G>C	p.Glu195Asp	31.11
	-					*CSMD1*	Splice	c.86-2A>G		26.09
	-					*BTG1*	Missense	c.136G>A	p.Glu46Lys	38.39
	-					*IGLL5*	Splice	c.206+1G>C		37.45
97	*PIM1*	Nonsense	c.720G>A	p.Trp240Ter	41.68	*PIM1*	Nonsense	c.720G>A	p.Trp240Ter	44.93
	PIM1	Nonsense	c.908G>A	pTrp303Ter	41.99	*PIM1*	Nonsense	c.908G>A	p.Trp303Ter	43.76
	GRHPR	Splice	c.287+1G>A		36.71	*GRHPR*	Splice	c.287+1G>A		47.28
	KMT2D	Frameshift	c.15891_15895dupGGTGC	p.His5299ArgfsTer8	37.80	*KMT2D*	Frameshift	c.15891_15895dupGGTGC	p.His5299ArgfsTer8	52.79
	CD79B	Missense	c.590A>G	p.Tyr197Cys	33.35	*CD79B*	Missense	c.590A>G	p.Tyr197Cys	37.82
	BTG2	Splice	c.142+1G>C		30.43	*BTG2*	Splice	c.142+1G>C		39.49
	MYD88	Missense	c.794T>C	p.Leu265Pro	33.06	*MYD88*	Missense	c.794T>C	p.Leu265Pro	47.34
	MPEG1	Nonsense	c.556C>T	p.Gln186Ter	29.55	*MPEG1*	Nonsense	c.556C>T	p.Gln186Ter	42.65
	PRDM1	Splice	c.291G>C	p.Glu97Asp	51.92	*PRDM1*	Missense	c.291G>C	p.Glu97Asp	78.68
	CDKN2A	Loss				*CDKN2A*	Loss			

	CDKN2B	Loss				*CDKN2B*	Loss			
	PIM1	Nonsense	c.652C>T	p.Gln218Ter	80.38	-				
	GRHPR	Splice	c.214+1G>A		41.75	-				
	ETV6	Loss				-				
	NFKBIZ	Gain				-				
	-					*PIM1*	Splice	c.356-9_357delCTTTCCTAGGC		29.60
	-					*MYC*	Missense	c.486G>T	p.Glu162Asp	48.26
	-					*STAT6*	Gain			
	-					*IGLL5*	Loss			

Abbreviations: AA, amino acid; CNS, central nervous system; VAF, variant allele frequency

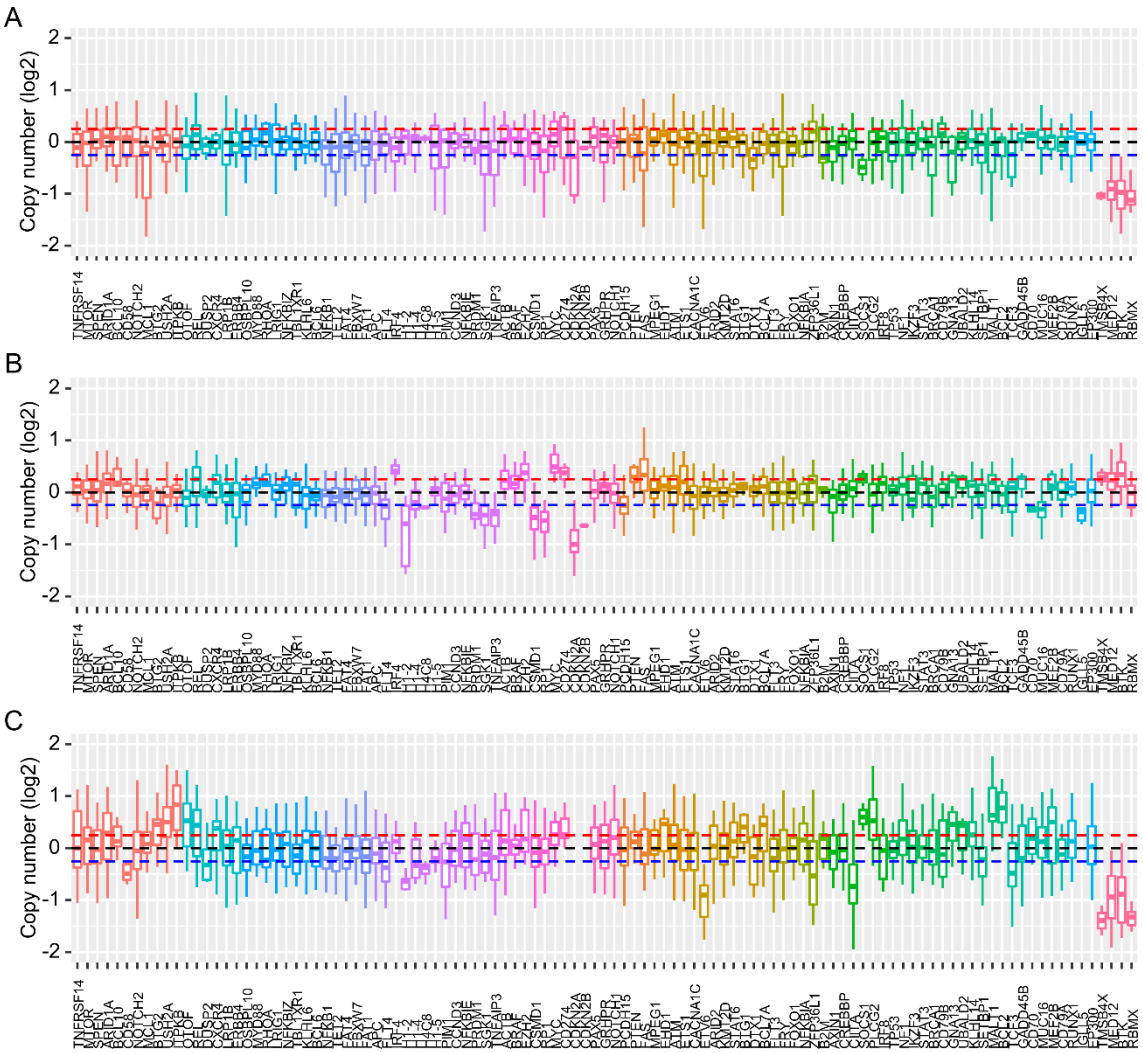

Supplemental Figure 1. Representative copy number plot. Copy numbers of each amplicon were shown as boxplot organized by the gene level. Results of uveitis sample (control) and two PVRL cases (Case 1 and 49) are shown in (A) and (B) and (C), respectively. Black dotted line indicates copy number neutral value. Red and blue dotted lines are thresholds for gain and loss, respectively.

Supplementary references

1. Levy N, Nelson J, Meyer P, Lukes RJ, Parker JW. Reactive lymphoid hyperplasia with single class (monoclonal) surface immunoglobulin. Am J Clin Pathol. 1983;80(3):300-308.
2. Bolger AM, Lohse M, Usadel B. Trimmomatic: a flexible trimmer for Illumina sequence data. Bioinformatics. 2014;30(15):2114-2120.
3. Li H, Durbin R. Fast and accurate short read alignment with Burrows-Wheeler transform. Bioinformatics. 2009;25(14):1754-1760.
4. Okonechnikov K, Conesa A, Garcia-Alcalde F. Qualimap 2: advanced multi-sample quality control for high-throughput sequencing data. Bioinformatics. 2016;32(2):292-294.
5. McKenna A, Hanna M, Banks E, et al. The Genome Analysis Toolkit: a MapReduce framework for analyzing next-generation DNA sequencing data. Genome Res. 2010;20(9):1297-1303.
6. Najima Y, Sadato D, Harada Y, et al. Prognostic impact of TP53 mutation, monosomal karyotype, and prior myeloid disorder in nonremission acute myeloid leukemia at allo-HSCT. Bone Marrow Transplant. 2021;56(2):334-346.
7. Talevich E, Shain AH, Botton T, Bastian BC. CNVkit: Genome-Wide Copy Number Detection and Visualization from Targeted DNA Sequencing. PLoS Comput Biol. 2016;12(4):e1004873.
8. Lohr JG, Stojanov P, Lawrence MS, et al. Discovery and prioritization of somatic mutations in diffuse large B-cell lymphoma (DLBCL) by whole-exome sequencing. Proc Natl Acad Sci U S A. 2012;109(10):3879-3884.
9. Wang X, Su W, Gao Y, et al. A pilot study of the use of dynamic analysis of cell-free DNA from aqueous humor and vitreous fluid for the diagnosis and treatment monitoring of vitreoretinal lymphomas. Haematologica. 2022;107(9):2154-2162.
10. Zhang F, Lu YJ, Malley R. Multiple antigen-presenting system (MAPS) to induce comprehensive B- and T-cell immunity. Proc Natl Acad Sci U S A. 2013;110(33):13564-13569.
11. Schmitz R, Wright GW, Huang DW, et al. Genetics and Pathogenesis of Diffuse Large B-Cell Lymphoma. N Engl J Med. 2018;378(15):1396-1407.
12. Challa-Malladi M, Lieu YK, Califano O, et al. Combined genetic inactivation of beta2-Microglobulin and CD58 reveals frequent escape from immune recognition in diffuse large B cell lymphoma. Cancer Cell. 2011;20(6):728-740.
13. Morin RD, Mendez-Lago M, Mungall AJ, et al. Frequent mutation of histone-modifying genes in non-Hodgkin lymphoma. Nature. 2011;476(7360):298-303.
14. Balinas-Gavira C, Rodriguez MI, Andrades A, et al. Frequent mutations in the amino-terminal domain of BCL7A impair its tumor suppressor role in DLBCL. Leukemia. 2020;34(10):2722-2735.
15. Lee J, Kim B, Lee H, et al. Whole exome sequencing identifies mutational signatures of vitreoretinal lymphoma. Haematologica. 2020;105(9):e458-460.
16. Bonzheim I, Sander P, Salmeron-Villalobos J, et al. The molecular hallmarks of primary and

secondary vitreoretinal lymphoma. Blood Adv. 2022;6(5):1598-1607.

17. Mlynarczyk C, Teater M, Pae J, et al. BTG1 mutation yields supercompetitive B cells primed for malignant transformation. Science. 2023;379(6629):eabj7412.

18. Hu N, Wang F, Sun T, et al. Follicular Lymphoma-associated BTK Mutations are Inactivating Resulting in Augmented AKT Activation. Clin Cancer Res. 2021;27(8):2301-2313.

19. Schmitz R, Young RM, Ceribelli M, et al. Burkitt lymphoma pathogenesis and therapeutic targets from structural and functional genomics. Nature. 2012;490(7418):116-120.

20. Kataoka K, Shiraishi Y, Takeda Y, et al. Aberrant PD-L1 expression through 3'-UTR disruption in multiple cancers. Nature. 2016;534(7607):402-406.

21. Davis RE, Ngo VN, Lenz G, et al. Chronic active B-cell-receptor signalling in diffuse large B-cell lymphoma. Nature. 2010;463(7277):88-92.

22. Nayyar N, White MD, Gill CM, et al. MYD88 L265P mutation and CDKN2A loss are early mutational events in primary central nervous system diffuse large B-cell lymphomas. Blood Adv. 2019;3(3):375-383.

23. Mottok A, Woolcock B, Chan FC, et al. Genomic Alterations in CIITA Are Frequent in Primary Mediastinal Large B Cell Lymphoma and Are Associated with Diminished MHC Class II Expression. Cell Rep. 2015;13(7):1418-1431.

24. Escudero-Esparza A, Bartoschek M, Gialeli C, et al. Complement inhibitor CSMD1 acts as tumor suppressor in human breast cancer. Oncotarget. 2016;7(47):76920-76933.

25. Treon SP, Tripsas CK, Meid K, et al. Ibrutinib in previously treated Waldenstrom's macroglobulinemia. N Engl J Med. 2015;372(15):1430-1440.

26. de Miranda NF, Georgiou K, Chen L, et al. Exome sequencing reveals novel mutation targets in diffuse large B-cell lymphomas derived from Chinese patients. Blood. 2014;124(16):2544-2553.

27. Bonetti P, Testoni M, Scandurra M, et al. Deregulation of ETS1 and FLI1 contributes to the pathogenesis of diffuse large B-cell lymphoma. Blood. 2013;122(13):2233-2241.

28. Gronbaek K, Straten PT, Ralfkiaer E, et al. Somatic Fas mutations in non-Hodgkin's lymphoma: association with extranodal disease and autoimmunity. Blood. 1998;92(9):3018-3024.

29. Laginestra MA, Cascione L, Motta G, et al. Whole exome sequencing reveals mutations in FAT1 tumor suppressor gene clinically impacting on peripheral T-cell lymphoma not otherwise specified. Mod Pathol. 2020;33(2):179-187.

30. Cai J, Feng D, Hu L, et al. FAT4 functions as a tumour suppressor in gastric cancer by modulating Wnt/beta-catenin signalling. Br J Cancer. 2015;113(12):1720-1729.

31. Liu N, Gao M. FLT4 Mutations Are Associated with Segmental Lymphatic Dysfunction and Initial Lymphatic Aplasia in Patients with Milroy Disease. Genes (Basel). 2021;12(10):

32. Trinh DL, Scott DW, Morin RD, et al. Analysis of FOXO1 mutations in diffuse large B-cell lymphoma. Blood. 2013;121(18):3666-3674.

33. Mai Z, Yuan J, Yang H, et al. Inactivation of Hippo pathway characterizes a poor-prognosis subtype of esophageal cancer. JCI Insight. 2022;7(16):

34. Muppidi JR, Schmitz R, Green JA, et al. Loss of signalling via Galpha13 in germinal centre B-cell-derived lymphoma. Nature. 2014;516(7530):254-258.

35. Andrades A, Alvarez-Perez JC, Patino-Mercau JR, Cuadros M, Balinas-Gavira C, Medina PP. Recurrent splice site mutations affect key diffuse large B-cell lymphoma genes. Blood. 2022;139(15):2406-2410.

36. Li H, Kaminski MS, Li Y, et al. Mutations in linker histone genes HIST1H1 B, C, D, and E; OCT2 (POU2F2); IRF8; and ARID1A underlying the pathogenesis of follicular lymphoma. Blood. 2014;123(10):1487-1498.

37. Cherian MA, Olson S, Sundaramoorthi H, et al. An activating mutation of interferon regulatory factor 4 (IRF4) in adult T-cell leukemia. J Biol Chem. 2018;293(18):6844-6858.

38. Reddy A, Zhang J, Davis NS, et al. Genetic and Functional Drivers of Diffuse Large B Cell Lymphoma. Cell. 2017;171(2):481-494 e415.

39. Choi J, Phelan JD, Wright GW, et al. Regulation of B cell receptor-dependent NF-kappaB signaling by the tumor suppressor KLHL14. Proc Natl Acad Sci U S A. 2020;117(11):6092-6102.

40. Pon JR, Wong J, Saberi S, et al. MEF2B mutations in non-Hodgkin lymphoma dysregulate cell migration by decreasing MEF2B target gene activation. Nat Commun. 2015;6(7953.

41. Weniger MA, Kuppers R. Molecular biology of Hodgkin lymphoma. Leukemia. 2021;35(4):968-981.

42. Dobashi A, Togashi Y, Tanaka N, et al. TP53 and OSBPL10 alterations in diffuse large B-cell lymphoma: prognostic markers identified via exome analysis of cases with extreme prognosis. Oncotarget. 2018;9(28):19555-19568.

43. Gu Z, Churchman ML, Roberts KG, et al. PAX5-driven subtypes of B-progenitor acute lymphoblastic leukemia. Nat Genet. 2019;51(2):296-307.

44. Zheng T, Zhou H, Li X, et al. RBMX is required for activation of ATR on repetitive DNAs to maintain genome stability. Cell Death Differ. 2020;27(11):3162-3176.

45. Koskela HL, Eldfors S, Ellonen P, et al. Somatic STAT3 mutations in large granular lymphocytic leukemia. N Engl J Med. 2012;366(20):1905-1913.

46. Yildiz M, Li H, Bernard D, et al. Activating STAT6 mutations in follicular lymphoma. Blood. 2015;125(4):668-679.

47. Venturutti L, Teater M, Zhai A, et al. TBL1XR1 Mutations Drive Extranodal Lymphoma by Inducing a Pro-tumorigenic Memory Fate. Cell. 2020;182(2):297-316 e227.

48. Kato M, Sanada M, Kato I, et al. Frequent inactivation of A20 in B-cell lymphomas. Nature. 2009;459(7247):712-716.

49. Wu F, Watanabe N, Tzioni MM, et al. Thyroid MALT lymphoma: self-harm to gain potential T-

cell help. Leukemia. 2021;35(12):3497-3508.